Strategies for Organic Food Waste to Power Conversion in a New Apartment Complex in Lagos, Nigeria

Akhilesh Bakshi
MechE - MIT
abakshi@mit.edu

Soufien Taamallah
MechE - MIT
sofiene@mit.edu

Kevin S. Kung
BioE - MIT
kkung@mit.edu

Abstract *The use of biomass and organic waste from households, industry and farms for energy conversion could contribute to sustainable development on several fronts, namely, environmental, social, and economic. It is widely considered as one of the solutions to lower the dependence on expensive imported energy sources and improve people's access to energy hence their quality of life, especially in rural areas, while potentially limiting greenhouse emissions. In developing countries, the use of organic waste for energy purposes can also alleviate reliance on diesel which is the default backup option when suffering from power supply intermittency. For instance, in Lagos, Nigeria, a new apartment building built, can expect electricity from the grid only during 2/3 of the day in average with random, non-planned shutdowns. The choice and overall effectiveness of a municipal waste and in general biomass to energy method depends on the feedstock composition and related heating value. Along with the form of energy needed (electricity, heat, or liquid fuel for transportation), the biomass characteristic will determine the suitable energy conversion method to be used. In the first phase of this study, we provided, through our midterm report, an extensive review of the biomass sources used for energy purposes and extracted the relevant parameters essential for a suitable choice of conversion method. This was complemented with the review of the different thermochemical and biochemical processes used today for biomass to energy purposes. In this final report, we analyze the case of a new apartment complex in Lagos Nigeria, as part of the project undertaken by NovaGen, a startup created at MIT with the goal to provide property managers with an alternative to diesel fuel for generators, while fostering waste reduction at source through waste to energy conversion. We revisited our literature review and selected the most promising thermochemical and biochemical method for our particular application. Based on simplified models built using ASPEN along with ultimate analysis-based correlations, we estimated the amount of electricity produced by the available waste along with the diesel fuel cost reduction.*

1 Introduction

Large-scale introduction of biomass energy could contribute to sustainable development on several fronts, namely, environmental, social, and economic [1]. World energy supplies have been dominated by fossil fuels for decades (approximately 80% of the total use of more than 400 EJ per year) [2]. Today biomass contributes about 10 to 15% (or 45 ± 10 EJ) of this demand. On average, in the industrialized countries biomass contributes some 9 to 14% to the total energy supplies, but in developing countries this is as high as one-fifth to one-third [3]. In quite a number of these countries, biomass covers even over 50 to 90% of the total energy demand. It should be noted, though, that a large part of this biomass use is noncommercial and used for cooking and space heating, generally by the poorer part of the population [4].

Nonetheless, in many parts of the developing world such as India and Nigeria, millions of tons of unmanaged organic waste is dumped into informal landfill or set on fire every day because there is a lack of perceived value for it, despite its great energy generation potential. In this study, we propose to assess the viability for energy conversion of such waste, given its broad potential applications in many parts of the world.

This document present the first phase toward that goal: we will first gain a better understanding of the nature of such waste through characterizing different types of biomass that may be present in the waste stream, and then give an overview of the potential energy conversion technologies that may be suitable for organic waste. Finally, we propose the research goals for the second phase of our project.

2 Background and Motivation

Lagos is the most populous city in Nigeria. It is today the largest city in Africa and the 7th largest urban area in the world according to the United Nation. Access to energy and in particular electricity is one of the challenges that Lagos faces. An important intermittency is associated with power supply to households. In average, electricity is not available for up to 8 hours per day (with a maximum of 16 hours per day) making necessary to have a complementary source of power. Very often, a diesel generator is used to provide power when the utility power is not available. Lagos, as most of large cities in the world faces also the challenge of household and municipal waste. Large quantities of waste are directed towards landfills. Organic waste, in particular food waste is a large part of this total waste. A study of global food waste published in 2011 by the Food and Agriculture Organization of the UN found that roughly one third of all food produced for human consumption each year goes to waste totaling 1.3 billion tonnes [5].

NovaGen NovaGen is a startup from MIT with the goal of providing more sustainable solutions for electricity intermittency in Lagos, compared to diesel, by taking advantage of the large mass of daily organic waste. NovaGen is doing a pilot study based on the case of a new apartment complex being built in Lagos.

3 Goal and Approach

NovaGen is seeking to enter the Nigerian market as a renewable energy provider for the urban apartment blocks (around 70 households), and is evaluating the options of biodigestion and gasification. The goal of our project is to provide NovaGen with an assessment, from the systems design and energy conversion perspective, which one of these two options may be more viable in the Lagos context. In particular, NovaGen is seeking to provide electricity to households only during hours of grid outage, which is estimated to be about 8 hours/day. The estimated household electricity consumption is around 3 kW (the confidence interval is, however, between 1.5 kW and 8 kW, as data are sparse).

The business as usual scenario for those households would be to burn diesel in diesel generators, and diesel, priced at about 160 Naira/L (USD 1/L), is relatively expensive. NovaGens value proposition is to provide a lower-cost source of electricity for these apartment blocks during hours of power outage. Insights from this study may help NovaGen devise an energy conversion method with better conversion efficiency.

In order to carry out this assessment, we will employ several multi-scale approaches for both energy conversion pathways. As a first step, we will carry out a brief literature review over the existing waste treatment technologies to understand why gasification and biodigestion may be two processes of choice for municipal waste on a small community scale. Then, we will model both processes at different scales. As an illustration, for gasification, we will develop a kinetics-based and single-particle approach to understand fuel production and composition. This detailed modeling will help us evaluate how potential fluctuations in the incoming feedstock characteristics will affect the fuel characteristics, and therefore, the system performance. We will then consider the energy balance inside the gasifier, and integrate the gasifier into an overall systems model that encompasses a dryer, gasification unit, and diesel engine in order to predict the system performance. We will undertake a similar approach for biodigestion. At the end, we will compare the outputs from both pathways, and make a recommendation about the better conversion pathway to pursue, at least from the energy conversion perspective. In order to achieve these goals, we will use a variety of modeling tools such as MATLAB, EES, Cantera, and ASPEN Plus based on existing models as well as values/parameters obtained from our the literature search.

The key question that we will first address is: Given the amount of municipal waste available in the apartment blocks (about 120 kg/day), does the organic fraction (57% by weight) of the waste suffice for power provision to fulfill the needs of the apartment block (around 3 kW for 8 hours/day)? Given that mixed municipal waste may be subject to significant daily and seasonal variations, how sensitive are our projected figures to fluctuations in the input feedstock characteristics? At the end, should NovaGen go ahead with its project, and if so, how much money can it save?

We recognize that because we are addressing the issue of power intermittency, energy storage is an important aspect of the project. However, due to the limited scope of this study, we focus our attention mostly on the energy balance of the waste-to-energy conversion process, and leave the issue of energy storage for further work.

The key data on the energy requirements for Lagos case is summarized below. The important data on municipal waste characteristics in Lagos were extracted from Amber et al. [6].

	Min	Avg	Max
Diesel Price	156	160	170
Electricity Consumption	1.5	3	8
Scale	20	70	210
Waste	-	0.5	-
People per household	2	6	-
Electricity Unavailability	4	8	16
Waste Composition	45% Vegetable, 8% Putrecables, 4% papers, 15% plastics, Glass 5%, Metals 5%, Textiles 10%, Fines 8%		
Electricity Cost	Fixed Charge: #1,688 per month Energy Charge: #12.87 per kWh		

Figure 1: Data for typical apartment complex in Lagos, Nigeria

4 Literature review and selected technologies

4.1 Thermochemical

4.1.1 Biomass Combustion

Biomass combustion is used to convert the chemical energy stored in biomass into heat, mechanical power or electricity. When heating biomass, its constituents start to hydrolyze, oxidize, dehydrate and pyrolyze with increasing temperature forming combustible volatiles, tarry substances and highly reactive carbonaceous char. At the ignition temperature, cellulose, hemicellulose, lignin and water vapor are stripped off and decompose into partial or complete combustion products in the flaming zone. The feedstock HHV depends on the combination of proximate, ultimate and structural analyses. For instance, the lignin content of the sample is strongly correlated with the heating value. While theoretically it is possible to burn any type of biomass, in practice combustion is feasible only for biomass with a moisture content $< 50\%$, in order to keep the combustion temperature (hence the combustion quality) and thermal efficiency high [7]. Biomass that has significantly high volatile components is easier to ignite (as compared to coal or torrified biomass), but the downside is that controlling ignition is a must while a longer high temperature zone must be maintained in order to

achieve complete combustion at high efficiency and to control emissions [8]. Finally, a high ash content in the biomass fuel makes it less desirable as a fuel [9]. This is because ash acts as a heat sink, in the same way as moisture, besides being responsible for corrosion, agglomeration and disposal issues adding to maintenance costs. Biomass combustion is mainly used for heat production in small and medium scale units and the selection of the furnace type is largely determined by the operating scale, fuel type and fuel residence time. Overall, combined heat and power (CHP) production uses biomass combustion in conjunction with steam cycles with typical power outputs in the range 0.5-10 MW_e. Net bio-energy conversion efficiencies for biomass combustion power plants range from 20% to 40%. The higher efficiencies are obtained with systems over 100 MW_e or when the biomass is co-combusted in coal-fired power plants [7, 10].

One of the big hindrances in using biomass as a fuel for direct combustion is the emission control, along with the combined nuisance of corrosion and agglomeration. Some of the major issues concerning the combustion process are as follows:

- *PAH Emissions*: Most of the five or six member ring Polycyclic Aromatic Hydrocarbons (PAHs) are formed as a result of chemical changes during combustion, some of them are known or suspected carcinogens [11]. The formation mechanism of PAHs is very complex and not completely known, but it is suggested that PAHs are formed by incomplete combustion during pyrolysis ($< 850°$C) and through synthesis reactions in the presence of oxidants OH, O_3, HNO_3 etc at high temperatures ($> 850°$C). To avoid PAH formation, air staging and oxygen-rich combustion are essential [8].

- *CO Emissions*: Like conventional fuels, CO formation is primarily due to incomplete oxidation, i.e. fuel-rich combustion or short residence time of the fuel. Biomass that has a higher volatile component ($\sim 75\%$) needs more residence time to completely burn the volatiles. The problem is further amplified by larger fuel particles (densification / pulverizing biomass is often expensive), higher ash content and moisture, which reduces the combustion temperature, thereby, slowing the oxidation kinetics.

- *NO_x Emissions*: Since most fluidized bed reactors operate at relatively low temperatures, typically $\sim 900°$C, formation of NO_x is primarily in the form of fuel NO_x, or to some extent, prompt NO_x. Typically, this is not a major concern since the nitrogen content in biomass is low while presence of char further assists in the reduction of NO_x emissions. Thus, even though char content in biomass is low, co-firing biomass with coal reduces the overall emissions. NO_x emissions can be primarily controlled by air and fuel staging, with rich burning in the first stage followed by stoichiometric combustion in the following stage. Since this introduces construction / control complexity, NO_x reduction may be done using selective catalytic reduction with ammonia, or by fuel reburning, the latter would, however, come at the cost of increase in CO/CO_2 emissions [8].

- *Particulates*: Particulate emission arises either from incomplete combustion (soot, tar and char) or from the inorganic material in the fuel. While the former is controllable by carefully selecting the operating conditions, the latter is a big menace in biomass combustion and is directly related to the chlorine and alkaline content in the fuel. Most of the particles are sub-micron scale [12], thus requiring efficient cleaning systems, unlike coarse particles (> 5 micron) which can be efficiently removed using cyclone and electrostatic precipitation filters [8].

- *Deposits, Corrosion and Agglomeration*: Presence of alkali metals (predominantly K) results in the formation of salts (silicates). Chlorine in the biomass sample increases the volatility of the alkali metals, releasing them as alkali chlorides and hydroxides in the gas phase which react with SO_2 to form low melting point silicates which stick to the surface. The non-volatile

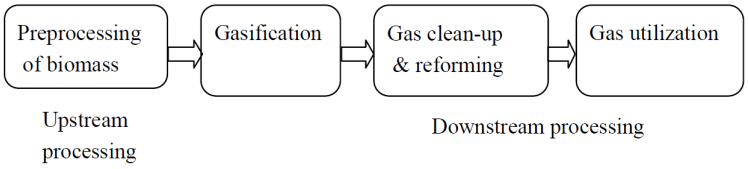

Figure 2: Schematic of Biomass Gasification Process [15]

compounds, by coalescence or melting, form ash particle which also remain at the bottom of the bed and cyclone system. Thus, all metal surfaces are either directly attacked by gas species (eg Cl_2) or corrode due to formation of solid / molten phase on the surface rendering the heat transfer process ineffective [9]. The latter can be mitigated by using materials such as bauxite, limestone, kaolinite etc which increase the melting point of alkali compounds, although chlorine is still released in the gas phase [13]. Similarly, in the combustion of biomass samples with high alkaline content (e.g. herbaceous biomass) agglomeration results when the ash released forms layers around inert particles. In fluidized bed, for example, this disrupts the bubbling phenomena, and in the extreme case, causes boiler defluidization [13, 14]. Co-combustion, fuel pre-processing and use of alternate bed material are strategies often employed, but with the subsequent flow and chemical stability issues appropriately addressed [8].

While direct combustion of biomass is presently a reliable, low-risk and flexible energy conversion technique, the biggest hurdle is the emission control: better combustor designs ensure check on CO and PAHs emissions, while post treatment for NO_x and particulates, but the challenge is related to the ash content which significantly reduces the life of all equipments in a biomass combustion system, and is also a menace with respect to disposal [13]. Keeping emission control in mind along with limitations on feedstock and product flexibility, gasification is often preferred over direct combustion.

4.1.2 Gasification

Gasification is the conversion of biomass into a combustible gas mixture by the partial oxidation of biomass at high temperature, typically 800-1000°C. The gas produced can be burned directly, used as a fuel for gas turbine / internal combustion engines or used in the production of fuels (e.g. hydrogen) or other chemicals (e.g. methanol). As shown in Figure (2), a gasification system is typically made up of three essential systems: (1) the gasifier, used to produce the combustible gas (2) the gas cleanup system and (3) the energy recovery system. Details regarding the gasifier and the energy recovery system are presented in the following sections.

Fundamentals: Gasification of biomass can generally be represented as

$$\text{Biomass} + O_2\,(\text{or}\,H_2O) \rightarrow \text{Producer Gas}\,(CO, CO_2, H_2, CH_4, N_2) + H_2O + \text{tar} + \text{char} + \text{ash} \quad (1)$$

$$CO + H_2O \leftrightarrow CO_2 + H_2 \quad \Delta H = -42\text{kJ/mol} \quad (2)$$

$$CO + 3H_2 \leftrightarrow CH_4 + H_2O \quad \Delta H = -88\text{kJ/mol}, \quad (3)$$

where the final composition is governed by the water-gas shift and methane formation reactions given by Equations (2) and (3). Char is the carbonaceous solid residue of biomass while tar is a complex mixture of condensible hydrocarbons which include single ring to complex polycyclic aromatic hydrocarbons (PAHs) [16], both being the result of incomplete conversion of biomass. In general, the producer gas composition is a function of fuel properties such as fuel composition and moisture content and operating parameters such as (1) gasifying medium (2) operating pressure (3) temperature (4) equivalence ratio (6) residence time (7) homogeneity in the reactor and (8) catalysts. Typical syngas compositions are listed in Figure (3).

Oxidant	Composition (vol%)					
	H_2	CO	CO_2	CH_4	N_2	LHV(MJ/Nm^3)
Air	9÷10	12÷15	14÷17	2÷4	56÷59	3÷6
Oxygen	30÷34	30÷37	25÷29	4÷6	-	10÷15
Steam/CO_2	24÷50	30÷45	10÷19	5÷12	-	12÷20

Figure 3: Typical syngas composition with different oxidants [17]

Fuel Requirements: The fuel moisture content typically has to be less than 15% before gasification since higher moisture reduces the temperature achieved in the oxidation zone, resulting in incomplete cracking of hydrocarbons. Thus, dryers are often employed using the waste heat from the system to dry the biomass fuel to acceptable moisture levels. Similarly, as in direct combustion, ash content in the feedstock must be checked to prevent slagging / fouling inside the gasifier, and thus physical / chemical separation methods (eg fractionation, leaching) may be used to restrict the ash content to less than 5%. Finally, the fuel must also be ground to small particle sizes (typically 20-80 mm) since large particles tend to form bridges and prevent effective movement of the fuel [18]. Therefore, the overall energy consumption during size reduction depends on the moisture content, initial biomass size, biomass properties and mill properties [15] and including the cost of biomass pre-treatment, this could contribute to as high as 50% of the total gasifier unit cost [18].

Table 1: Main advantages and technical challenges of various operating conditions

	Advantages	**Technical Challenges**	**References**
Gasifying Agents			
Air	Heat requirement for gasification met Moderate char and tar content	Low heating value (3-6 MJ/Nm^3) Large amount of N_2 in syngas	[18, 19]
Steam / CO_2	High heating value syngas H_2-rich syngas (>50% volume)	Indirect or external heat supply Catalytic tar reforming required	[20, 21]
Gasifier Design			
Fixed/Moving Bed	Simple, reliable design Favorable economics on small scale	Non-uniform temperature High char and/or tar content	[18, 22]
Fluidized beds	Short residence times Uniform temperature distribution	High particulate dust in syngas Catalytic tar reforming required	[18, 22]
Gasifier Operation			
Temperature increase	Decreased char and tar content Increased heating value of syngas	Decreased energy efficiency Increased ash related problems	[19, 23]
Pressure increase	Low char and tar content No syngas compression cost	Limited operation experience Higher cost at small scale	[18, 22]
ER increase	Low char and tar content	Decreased heating value of syngas	[24]
Catalyst			
Naturally occurring (dolomite, olivine)	Cheap	Moderate reforming efficiency Easily eroded and broken	[25, 26]
Alkali salts	High reforming efficiency Increased Hydrogen in syngas	Increased plugging/slagging and destabilization of metal catalysts	[25, 27]
Stable metal oxides	High reforming efficiency Increased Hydrogen in syngas	Expensive Deactivated by coke, sintered by ash	[25, 28]

Operating Conditions and Process Challenges: Table (1) highlights the main operating parameters. Broadly, there are two types of gasifiers, fixed bed and fluidized bed. Fixed bed gasifiers have

been traditionally used and operate at about 1000°C. Fixed bed gasifiers are the most common small scale-gasifiers and are predominantly updraft or downdraft gasifiers. Updraft gasifiers are counter-current gasifiers where the feedstock is loaded from the top while air is introduced from the bottom of the reactor. Thus, the feedstock typically undergoes the following processes (in order): drying, pyrolysis, reduction and combustion. As the air moves up, it carries the tar produced in the pyrolysis zone upwards and since the temperature decreases moving upwards, the tar content freezes resulting in the production of gas with high tar content. On the other hand, in a downdraft gasifier, the feedstock is introduced at the top, while air is introduced through the sides above the grate and the combustible gas is withdrawn under the grate. As a result of this configuration, tar is effectively cracked as it moves through the high temperature combustion zone. On the downside, the internal heat exchange is not as efficient as in an updraft gasifier. In addition, fixed bed gasifiers are usually limited in scale (0.15-1 MWe) and must be fuel-optimized, making them rather fuel-inflexible [16]. Meanwhile, fluidized bed gasifiers are fuel-flexible (catalysts can also be added) and are able to maintain uniform temperature/mixture homogeneity by using high specific heat fluidizing media such as silica and alumina materials [15]. However, the upper limit on the temperature (800-1000 °C) is set by the melting point of the bed material, which is also why these are unsuitable for coal gasification due to lower reactivity of coal at temperatures less than about 1300 °C. Fluidized bed gasifiers and in particular, circulating beds, are ideal for fuel capacity higher than thermal 10 MW [16].

Supplying steam as a gasifying agent increases the partial pressure of water and hence, favors hydrogen formation (water-gas shift). The downside, however, is that this reaction is endothermic, requiring external or internal (via biomass oxidation) heat source or presence of catalysts to drive the reaction forward. Recently, although not commercialized, gasification using plasma and supercritical water are also being explored as possible options since they also provide for effective waste removal [29, 30].

One of the biggest concerns with gasification systems is tar condensation at temperatures below 450°C which gets deposited along the piping walls and partly as an aerosol in the gas. The tar content, thus, hinders the removal of particulate emissions as the subsequent utilization of the gas [31]. The properties of this tar itself varies based on the operating condition; for instance, air gasification produces viscous tar, while steam gasification produces low-molecular-weight liquid tar [18]. Tar may be cracked by operating the gasifier at elevated temperatures 900-1100°C [24], but since this high temperature requires more combustion, the efficiency decreases and hence, catalysis at the usual gasification temperature 800-900°C is preferred [16, 18, 22]. Another technique is to use electrostatic precipitators to capture aerosols after cooling the gas to 60-80°C [18, 31].

Applications: Some of the major (potential) applications of biomass gasification are :

- *CHP*: This has conventionally been the primary application for gasification. Several commercial plants have been set up ranging from 20 kW in the Amazon region (for local needs) [24] to 6 MW electricity (+ 9 MW thermal) from wood chips in a village in Sweden [15]. Overall efficiencies of up to 35-40% have been reported [15, 22]. Currently, India generates about 70 MW of electricity from small-scale biomass gasification systems (for example, Husk Power), which is about 70% of the basic energy needs in the rural areas [24]. There are several studies in light of this from both from the energetics as well as the economics point of view (e.g. [32, 33]).

- *Hydrogen Production*: Gasification can be used for producing hydrogen as a transportation fuel since it has better combustion properties than conventional fuels [16]. A combination of catalysts can be used to drive the water reforming and water-gas shift reaction (e.g. Cu-Zn) in favor of H_2 and CO_2 production. Subsequently, the CO_2 may either be adsorbed (e.g. by

CaO) or sequestered downstream to yield pure hydrogen [22]. Compared to other techniques for hydrogen production, gasification remains a subject to ongoing research [24].

- *Ethanol production*: The biggest advantage of biological conversion over chemical catalysis is that most anaerobes are sulfur-tolerant (and hence, do not require expensive sulfur cleaning technology) and not sensitive to CO/H_2 ratio (and hence, fuel flexible) [22]. However, the major challenge with this process is to increase the rate and yield of fermentation by increasing gas to liquid mass transfer of CO and H_2 and to search for the right microbe having a high resistance to the other contaminants in syngas [15]. Similarly, there has also been considerable research in deriving biodiesel through Fischer-Tropsch Synthesis and bio-methanol [16]. Although these derived fuels are shown to be cleaner than their conventional counterparts, low cost of petroleum-based feedstock makes their production uneconomical so far [15].

4.2 Thermochemical

As we saw in the first phase of this study, the two main biochemical process for biomass to energy conversion are fermentation and anaerobic digestion. Fermentation require relatively simple carbohydrate chains to be effective, and lead then to a liquid fuel mainly ethanol. Fermentation of lignocellulosic material like the ones found in organic food waste is more complex as it require hydrolysis and other conditioning steps to increase fermentability. Fermentation of lignocellulosic material is still in research and development. In contrast, anaerobic digestion is a well-established technology and has been commercially proven. It is Suitable for small and large scale, rural and urban areas and known to be attractive GHG mitigation option. A major advantage of anaerobic digestion in the specific case of food waste is the presence of not only carbohydrates in the food waste but also proteins and fatty materials all anaerobically biodigestable whereas during fermentation only carbohydrate are potentially processed. Anaerobic biodigestion has also advantages compared to composting as the latter method's output is predominately carbon dioxide which has no energy value. Moreover, cooked and oily food are suitable for biodigestion which is not the case for composting.

Table 2 shows the strengths and weaknesses for each of the main biochemical to energy conversion methods (biodigestion and fermentation).

Anaerobic digestion seems more suitable for food waste especially that we are interested in a technology readily applicable. Similarly, gasification seems the most suitable among thermochemical process. For all these reasons, we choose to pursue our analysis using anaerobic digestion and gasification as the two potential strategies. The scenarii we modeled and analyzed are shown in table 10.

Table 3: Different scenarii for electricity generation

Scenario	Energy source	Energy conversion
Business as usual	Diesel	Diesel engine
scenario 1	Food waste	Anaerobic digestion and Diesel engine
scenario 2	Food waste	Gasification and Diesel engine

5 Modeling

5.1 Gasification Process Modeling

In this section, we develop a quantitative multi-scale model for gasification, by considering the chemical kinetics, single-particle mass/heat transfers, gas-phase reactions, and finally, the system performance. Because we are interested in the sensitivity of the gasification process on the initial biomass,

Table 2: Summary of biochemical biomass to energy conversion

Method	Energy form	Strength	Weakness
Anaerobic Diges.	Biogas	- Well-established tech. - Commercially proven - Widely applied for homogeneous wet organic waste streams and waste water. - Suitable for small and large scale, rural and urban areas. - Attractive GHG mitigation option	- To a lesser extent used for heterogeneous wet wastes such as organic domestic wastes (sorting required)
Fermentation (1^{st} gen.)	Bioethanol	- Straightforward sugar fermentation	- Competition with food - If applied to organic waste, only carbohydrate will be converted - Varying GHG abatement potential
Fermentation (Cellulosic-2^{nd} gen.)	Bioethanol	- Abundant resource - Clear GHG abatement potential	- Pretreatment and hydrolysis required

it will be important for us to predict, with reasonable detail, the major species that emerge from the gasifier. This necessitates the use of a detailed chemical kinetics mechanism. The results from this sensitivity study will be later used to model the larger gasifier system.

The reactor model—which incorporates the detailed kinetics and single-particle mass/energy transfer effects—roughly consists of two parts: the initial solid-phase drying and devolatilization reactions, and the latter gas-phase combustion and gasification reactions. In this section, we will describe these two models separately as they primarily concern themselves with the different phases.

5.1.1 Gasifier Design

Considering the scale of operation (<20 kWe), an air blown downdraft gasifier is chosed for the present study. A typical downdraft gasifier and its schematic is shown in Figure (4). As was highlighted before, the advantage of a downdraft gasifier is that the product gases leave the gasifier at a high temperature (800-1000°C) enabling partial cracking of tars formed during gasification, however, at the cost of an efficiency penalty associated with the high heat content of the product gases [18]. Its popularity can be gauged by various studies in literature using a huge range in feedstock including wood [34, 36–39], sugarcane leaves [40] and sewage sludge [41] operating in the range 5 kWe - 80 kWth.

Modeling : In general, there are two broad approaches for modeling fixed bed gasifiers: thermodynamic equilibrium models and kinetic models. Thermodynamic equilibrium models are based on a steady state analysis and hence, may not predict in good agreement with experiments for operating

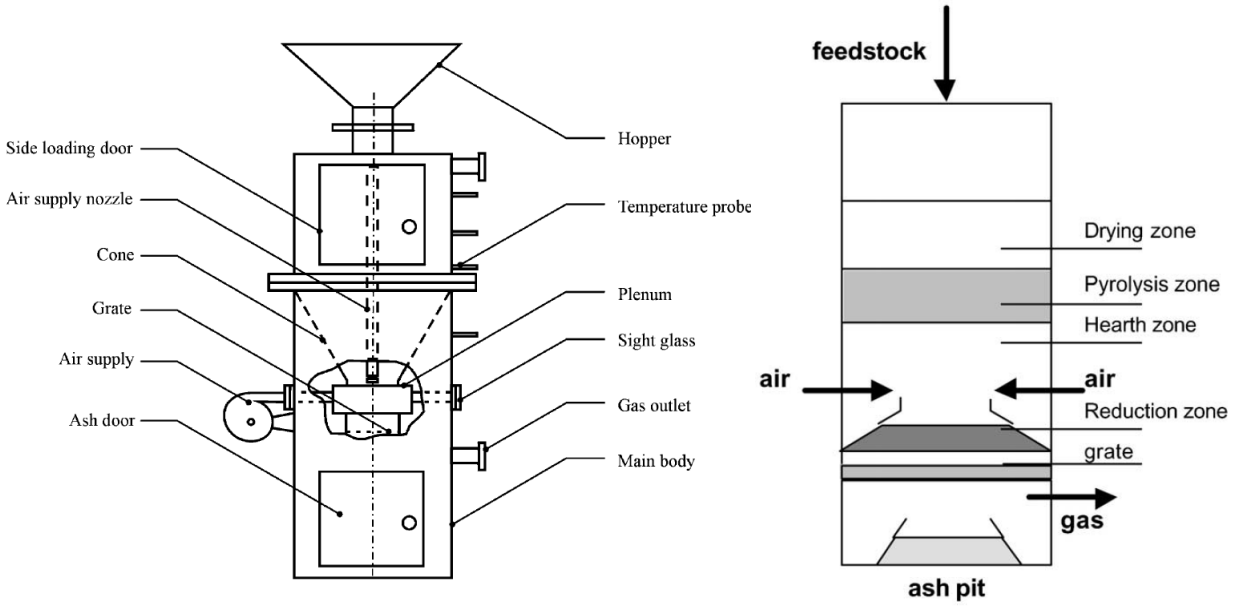

Figure 4: Experimental facility [34] and schematic [35] of a typical downdraft gasifier

temperatures lower than 1000°C, where reactions tend to be more kinetic controlled and hence, do not reach equilibrium. Other typical assumptions include [42]:

- Reactor is implicitly zero-dimensional
- Perfectly insulated apparatus i.e. heat losses are often neglected, although this can be easily incorporated into the model
- Perfect mixing and uniform temperature throughout the gasifier, which is almost never possible in practice
- Usually no information on the reaction intermediates is given

The equilibrium model assumes a given operating temperature and solves for the product composition based on mass balance equations and thermodynamic equilibrium equations, including temperature dependent equilibrium constants for the water-gas shift and methane formation reactions. Additionally, empirical constants may be included to the equilibrium calculations to fit the model output with experimental data (e.g. [43]). While typically not included, some studies (e.g. [44]) have considered tar even though the composition and formation mechanism of tar are somewhat empirical. Considering the limited applicability of these models, thermodynamic equilibrium models are, thus, more suitable for parametric studies.

Meanwhile, kinetic models provide a more mechanistic insight into the conversion process. While these rate models are accurate and detailed, the complete mechanism often needs to be simplified due to computational constraints. Nevertheless, the char reduction process may be accurately determined using experimentally obtained rate expressions for short residence times of gas and biomass [42]. Tinaut et al [39] analyzed the impact of biomass (pine bark) particle size and superficial gas velocity on the steady state gasification process by implementing an exhaustive kinetic model including both the gas-phase and heterogeneous reactions in all the four gasifier zones. As a simplification to the full-scale model, Giltrap et al [45] developed a model for the reduction zone in a gasifier by considering mass and energy balance along the reduction zone using four given parameters: gas concentration and temperature into the reduction zone (from the combustion zone), char reactivity factor

(CRF) accounting for the porous structure, and hence, the reactivity of char and the pyrolysis fraction representing the effective fraction of initial gas that comes from the pyrolysis and cracking reactions. Building onto this model, Babu and Sheth [46] assumed a variable CRF (linear and exponential decrease) along the reduction zone to make the model more realistic as opposed to uniform CRF as imposed by Giltrap et al. Jayah et al [47] additionally used the *flaming pyrolysis zone* sub-model to predict the gas composition and temperature which was then fed as an input to the gasification zone sub-model. While a lot of these models are application specific and experimental data dependent, kinetic models, in general, are more flexible than equilibrium models.

For the present study, a single-particle model has been used for char devolatilization. For the gas-phase reactions, especially during combustion, we employed the Ranzi gas-phase model, which consists of 450 species and 16,000 reactions. This kinetic scheme was made into a Cantera object, which was manipulated in MATLAB in order to integrate into the gasification reactor. For the gasification process, in addition to the gas-phase reactions as described above, there are also heterogeneous char-gas reactions. This is modeled in the Ranzi scheme [48] in Table 4 below.

Table 4: Heterogeneous char-gas reaction kinetic scheme, from [48]

Reactions	Reaction rate (kmol s^{-1})
Char + $O_2 \rightarrow CO_2$	$1.2 \times 10^{10} \exp(-32000/RT)$ [Char][O_2]
Char + 0.5 $O_2 \rightarrow$ CO	$2.5 \times 10^{11} \exp(-38200/RT)$ [Char][O_2]$^{0.78}$
Char + $H_2O \rightarrow$ CO + H_2	$2.5 \times 10^{9} \exp(-52000/RT)$ [Char]$^{0.5}$[H_2O]$^{0.70}$

In the case above, [Char] refers to the ratio of the current char to the initial char concentration, so it has a dimensionless range of between 0 and 1.

Choosing Parameters : The single particle model discussed above requires several input parameters so that the output gas composition can be calculated. This includes feedstock properties such as the composition which are known *a priori* while the operating conditions including particle diameter, temperature profile in the zones and the solid and gas residence times need to be estimated based on studies in literature. A compilation of some of the data presented in literature is presented in Table (5). While some data presented has been estimated / inferred based on the limited data provided in these studies and may not be accurate, these studies do provide a sense of typical data that may be used to design a hypothetical gasifier operation. Moreover, the methodology used in the current analysis can be easily extended when more accurate data is obtained.

The parameters required for the kinetic modeling are:

- **Reactor Geometry :** Based on the dimensions of most small scale reactors (5 kWe - 80 kWth) reported in literature, the gasifier used in the present study has an internal diameter of 0.5 m and length of 1 m.
- **Particle Diameter :** In case of large biomass particles, the gasifier section must be long for maximum conversion while for smaller particles, faster consumption (higher throughput) is possible [39, 47]. The disadvantage with smaller particles, though, is the higher cost required for grinding upfront. Thus, the particle size is typically based on the gasifier size although this must not exceed $1/8^{\text{th}}$ of the reactor diameter to avoid bridging effects [41, 47]. Keeping this in mind, the particle diameter used for this analysis is 5 cm, mainly to keep the grinding costs to a minimum considering the operating scale of this study.
- **Input Moisture :** Moisture content in the biomass affects both the gasifier operation as well as the quality of the gas produced. This is because for higher moisture content the energy

Table 5: Summary of operating conditions in literature (estimates have been provided if data not directly listed)

Study	Reactor (mm)	Feedstock	d_p (mm)	Residence Time		Gas Composition (% vol)				
				Gas	Solid	CO	H_2	CO_2	CH_4	N_2
Experiment										
[38]	300x1092	Rosewood (49C+6H+45O)	25.4	10-15 s	10-15 hr	15-22	7-12	4-8	1-2	59-68
[36]	2090 (ht)	Kiker wood	36	5-10 s	7-15 hr	18-23	10-11	5-20		50-65
[34]	600x2000	Wood (47C+6H+45O)	50	10-20 s	2 hr	23-25	13-15	12-14	2-3	44-46
[40]	300 (ID)	Sugarcane Leaves (40C+6H+47O)	10-100		15 min					
[41]		Sewage Sludge (40C+6H+26O)	10-35			6-11	9-11	11-13	1-2	62-64
Modeling (Equilibrium)										
[43]		MSW (51C+7H+40O)				18-20	12-17	8-12	1-2	51-60
[49]		Sawdust (52C+6H+42O)				20	14	12	2	51
Modeling (Kinetic)										
[39]	50x700	Pine Bark (55C+6H+38O)	2-19	5 s	1 hr					
[45]		Douglas Fir Bark (35C+10H+55O)				23-25	10-15	9-11	1-2	48-52
[47]	920x1150	Rubber Wood (51C+6H+42O)	33-55		10-15 hr	18-22	9-11	11-13	1-2	50-59

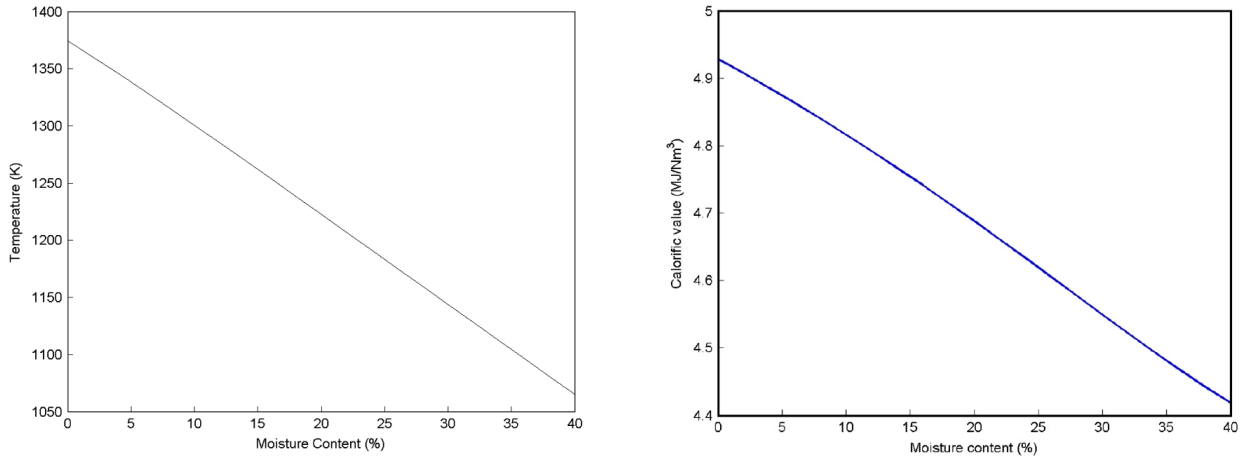

Figure 5: Effect of moisture content on the gasifier operating temperature and CV of the output gas [43]

requirement for drying increases which leads to a decrease in the gasifier operating temperature. In other words, with a higher moisture content, more air must be pumped in to maintain the operating reaction temperature reducing the mole fraction of the useful gases and hence, the calorific value. Jarungathammachhote and Dutta [43] used a modified equilibrium model to study the impact of moisture on the gasification of MSW in Thailand on both the operating temperature as well as the calorific value of the output gas, as shown in Figure (5). Based on their study as well as other reported literature, gasification of biomass with moisture content more than 40% is considered infeasible although in practice, it is usually less kept below 20% on a dry basis [38, 39, 43, 44, 47]. For the present study, the biomass entering the gasifier has 15% moisture (wet basis) and any additional moisture is removed using an external dryer.

- **Residence Time :** The residence time of the gas and solid phases was decided based on literature values. As can be seen in Table (5), the biomass / char residence time is typically in the order of hours while the gas residence time is much smaller (in seconds). Note that the values presented are only estimates and an accurate residence time, especially for gas / volatiles, can only be known if the exact experimental details regarding the geometry and the flow are known. For the present study, the solid and gas residence time have been fixed as 8 hrs and 4 s respectively.

- **Temperature Profile :** In the gasifier, peak temperature is achieved in the combustion zone where oxygen is supplied for partial combustion of the fuel to meet the energy requirements of the bed (gasification reactions are endothermic). While the combustion zone temperature itself depends on the equivalence ratio, the temperature in this zone is typically around 1000°C. Similarly, as reported in literature, typical temperatures in the drying, pyrolysis and gasification zones are 200°C, 400-500°C and 700-900°C respectively [38, 41, 50]. For the present study, a temperature profile is required as an input to evaluate the heat transfer in the single particle model. Therefore, as a first approximation, the gasifier has been primarily divided into two sections: (a) drying + pyrolysis zone at an average temperature of 400°C and (b) reduction zone at an average temperature of 800°C. The drying-pyrolysis zone has been fixed to be 0.6 m long, while the reduction zone occupies the bottom 0.4 m of the bed. The length of these zones should be verified post simulation to ensure that the drying-pyrolysis and reduction zones are long enough for the respective products to reach quasi-steady state. If this is not the case, several iterations will be required, as demonstrated in [47]. Meanwhile, combustion is assumed to take place in a narrow zone ($\sim$ 1 mm) between these two sections at a temperature of 1000°C

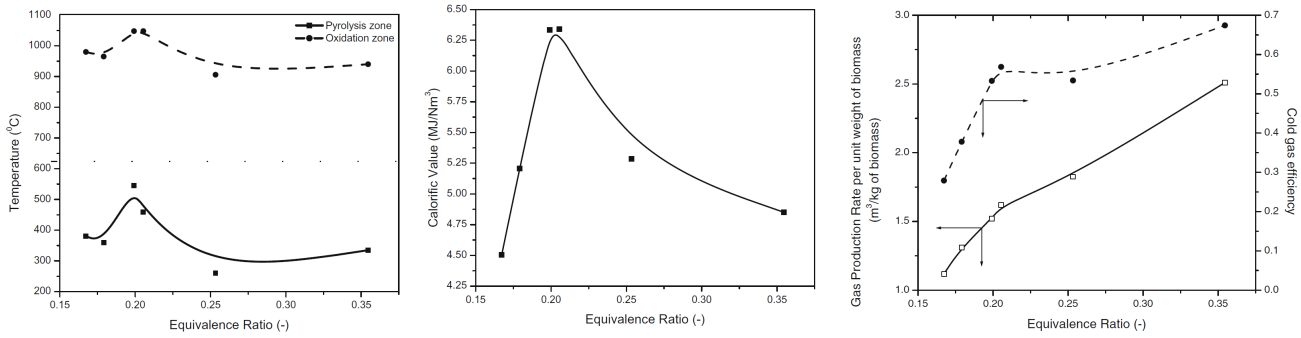

Figure 6: Effect of Equivalence Ratio on various operating conditions [38]

and as in the case of the other zones, it must be ensured that with the given gas and solid residence times, the oxygen supplied (in the air) is consumed completely before the gas / char enter the reduction zone.

- **Equivalence Ratio :** As mentioned before, since the gasification reactions are overall endothermic, some fuel must be burnt in air to meet the energy requirements of the gasifier unit. The flow rate of air pumped in is usually represented by the equivalence ratio ϕ given in terms of the air-fuel flow ratio A/F as

$$\phi = \frac{(A/F)_{actual}}{(A/F)_{stoich}} \tag{4}$$

Thus, gasifiers usually operate with $\phi < 1$ (fuel rich). While the actual value of ϕ employed depends on the feedstock and the absolute flow rates, a range of 0.25-0.5 is reported in literature [24, 39, 51]. Typically, for a given geometry and biomass flow rate, the equivalence ratio is optimized as shown in Figure (6). An initial increase in ϕ results in an increase in the CO_2 production in the combustion zone which results in an increase in the formation of CO and H_2 in the reduction zone and hence, an increase in the CV of the gas. At higher values of ϕ, however, CO_2 starts to accumulate in the system resulting in a lower CV of the gas. While Sheth and Babu [38] determine the optimal ER to be 0.205, other optimal values reported in literature include 0.276 [41] and 0.388 [34], highlighting the range of optimal ER that is possible. For this study, the ER ratio has been set as 0.2, though ideally, this must be optimized.

Gasifier Heat Requirement : While the oxygen (air) supplied must ideally be sufficient to meet the heat requirements of the gasifier, an alternate approach is to burn less biomass but supply external heat. Using this approach has a two-fold advantage: the producer gas has less Nitrogen content (and hence, a higher mole fraction of combustible gases CO and H_2) while it also provides an avenue to use the excess sensible heat (high quality) of the producer gas (or engine exhaust) effectively. However, such an approach may make the system layout complicated and hence, may not be feasible from a practical perspective.

In order to calculate the heat requirement of the gasifier (overall gasification reactions are endothermic), the gasifier unit is treated as a black-box and an enthalpy balance is performed between the inlet and outlet streams to determine the heat requirements of gasifier, in addition to the heat supplied by partial combustion of biomass. The calculation has been performed in EES and the code has been attached in the Appendix for reference. The steps in this calculation are:

1. The exit gas / char composition is calculated based on the Cantera single-particle model.
2. Based on the ultimate analysis of the biomass feedstock, its formula is determined as $CH_{1.58}O_{0.45}N_{0.02}S_{0.01}$. Mass balance across the gasifier is used to calculate the char composition.

3. The HHV of biomass and char is evaluated using the Boie equation [52] following which the heat of formation at standard condition is calculated based on the enthalpy of the following reaction [53]

$$CH_xO_y(s) + \left(\frac{2 + x/2 - y}{2}\right) O_2(g) \rightarrow \frac{x}{2} H_2O(l) + CO_2(g) \tag{5}$$

4. Since the gasifier output is at 800°C, the enthalpy of char at the gasifier temperature is obtained using $h_f^0 + \bar{C}_p \Delta T$, where the average specific heat capacity $\bar{C}_p$ between standard condition and the gasifier temperature and is evaluate using the expression in [53]

5. Finally, the heat required by the gasifier is simply the enthalpy difference between the reactants (biomass + moisture + air) and the products (gas + char) and is 8.33 kW for the present study.

5.1.2 Drying and Pyrolysis

In the first stage of the process (the first 60 cm of the reactor), we describe the devolatilization of the biomass. In this section, we assume that the air is inert, such that no oxygen is present. While this inertness is in practice is difficult to achieve completely, our gasifier design—with only the solid feed and without an air stream from the top of the reactor—at the least emulates this condition.

Mass Balance In our case, because the biomass particles are ground to a size of 5 cm immediately before gasification, it will be important to consider the conductive/convective effects within the particle. To do so, we utilize a single biomass particle model described in Bates and Ghoniem [53]. In this model, the solid-phase mass balance for ith species is described by

$$\frac{\partial \rho_i}{\partial t} + \vec{\nabla} \cdot (\rho_i \vec{v_i}) = \dot{w}_i. \tag{6}$$

It was noted by Bates and Ghoniem, by a scaling analysis within the single particle, that once devolatilized, the gas quickly convects out of the particle, and therefore we neglect the diffusion term inside the particle. Assuming no net accumulation of devolatilized gas, we have, for the gas phase,

$$\vec{\nabla} \cdot (\rho_i \vec{v_i}) = \dot{w}_i. \tag{7}$$

Assuming radial symmetry and integrating both sides, we obtain

$$\rho_i v_i = \frac{1}{r^n} \int_0^r r'^n \dot{w}_i(r') dr', \tag{8}$$

where n reflects the geometry of the particle: it is 0 for a flat plate, 1 for a long cylinder, and 2 for a sphere. In our case, we assume that our particles are spheres.

Energy Balance With radial symmetry and incompressible flow, we can write the energy balance as:

$$\sum_i c_{p,i} \rho_i \frac{\partial T}{\partial t} = \frac{\partial T}{\partial r} \left(\frac{\partial \langle k \rangle}{\partial r} + \frac{n \langle k \rangle}{r} - \sum_{i \in \text{Gas}} \rho_i v_i \right) + \langle k \rangle \frac{\partial^2 T}{\partial r^2} - \sum_i \dot{w}_i H_i. \tag{9}$$

Assuming known reactor temperature T_{react} = 400°C, the boundary conditions are given as follows:

$$T(r,0) = T_0, \tag{10}$$

$$\left.\frac{\partial T}{\partial r}\right|_{r=0} = 0, \tag{11}$$

$$\left.\frac{\partial T}{\partial r}\right|_{r=R} = h_c(T_{\text{react}} - T) + \omega\sigma(T_{\text{react}}^4 - T^4), \tag{12}$$

where the first right-hand term of Eqn. (12) reflects convection, and second right-hand term reflects radiation at the surface of the biomass particle. Therefore, h_c refers to the convective heat transfer coefficient, ω the emissivity coefficient, and σ the Stefan-Boltzmann constant.

Devolatilization Kinetics For the kinetics of the solid-phase devolatilization reaction, we utilized the Ranzi mechanism as described in [48]. In this mechanism, the biomass is considered to be made up of lignin, hemicellulose, and cellulose components, each undergoing a different set of devolatilization reactions. For example, cellulose first decomposes into activated cellulose, which then follows two different pathways of different kinetic rates to form large organic molecules or to form water and char. This 25-reaction, 45-species mechanism was programmed into Cantera, which ran on MATLAB in order to predict the dynamics of the devolatilization process. This mechanism is also able to predict the heat of reaction. In fact, when run at a surrounding temperature of 400°C, we determined that the reaction is slightly endothermic, at 776.87 kJ/kg of biomass.

Drying Kinetics Because drying is an important first step of the gasification reaction, we also sought to describe the process in reasonable detail by using an existing MATLAB model developed by Kevin Kung as part of his thesis research for thermally thick biomass.

In this model, drying is considered as the conversion of water from the "bound" to the "unbound" state:

$$\mathrm{H_2O_{(b)}} \longrightarrow \mathrm{H_2O_{(ub)}}. \tag{13}$$

The rate of drying is related to the amount of energy available. In other words, once the temperature has reached the local bound water-vapor equilibrium at temperature $T = T_{\text{Vap}}(\rho_b)$ (using experimentally measured correlations such as [54]), any excess energy flowing into the locality is used to evaporate water, before causing any further temperature rise:

$$\frac{\partial \rho_{\text{b}}}{\partial t} = \frac{1}{\Delta H_{\text{Vap}}} \max\left(0, \vec{\nabla}\cdot(k_{\text{eff}}\vec{\nabla}T) - \vec{\nabla}\cdot(Tc_{p,\text{ub}}\vec{\Phi}_{\text{ub}})\right), T > T_{\text{Vap}}(\rho_{\text{b}}). \tag{14}$$

This model found a reasonable fit with the experimental biomass drying data from Alves and Figueiredo [55], as well as from van der Stelt [56].

5.2 Biodigestion Process Modeling

Modeling a biodigestion system can be very complex but a minimum of three steps have to always be accounted for. First, the pre-treatment of the biomass prior to digestion. Many pretreatment methods exist as we will see later, but one of the main goals is to increase the surface area and the availability of the biomass for digestion, i.e. breaking large carbohydrate polymer to simpler sugars. This biomass conditioning is followed by the biodigestion step itself. Finally, a gas separation step is required to remove toxic and corrosive H_2S as well as the water contained in the biogas.

5.2.1 Pretreatment

The inherent properties of native lignocellulosic materials make them resistant to enzymatic attack. The aim of pretreatment is to change these properties in order to prepare the materials for enzymatic degradation. Taherzadeh et al. [57] published an extensive review of pretreatment technologies for biogas production. Various pretreatment methods exist for biodigestion : mechanical, thermal, chemical, ultrasonic and thermochemical pretreatments. These methods allow for an increase in productivity due to solubilization (hydrolysis) enhancement and particle size reduction. A comparison of different pretreatment technologies in terms of removal of hardly digestible components like lignin and hemicellulose, toxicity, inhibition of the biodigestion and finally cost has been made by Heidi Berg and shown in Fig. 7. Size reduction of biomass has also been found to reduce the retention time i.e. reduce the digestion time [**?**]. In our analysis, as we are assuming steady state, we are mainly interested in improvement in biodigestion yields i.e. the amount of chemical energy recovered in the output biogas as compared to the chemical energy available in the biomass.

Pretreatment Technologies Evaluated for Anaerobic Digestion

	Pretreatment Technology	Lignin Removal	Hemicellulose Removal	Inhibitors	Toxics	Economic Feasability	Source
Physical	Milling	Poor	Medium	Low	Low	Medium	M.J. Taherzadeh, 2008, A.T.W.M. Hendriks, 2008
	Irradiation	Good	Poor	Medium	Low	Poor	M.J. Taherzadeh, 2008
Thermal	Steam Pretreatment	Poor	Good	Medium	Low	Good	A.T.W.M. Hendriks, 2008
	Steam Explosion	Medium	Good	High	Low	Medium	M.J. Taherzadeh, 2008
	Liquid Hot-Water	Medium	Medium	Low	Low	Good	M.J. Taherzadeh, 2008, A.T.W.M. Hendriks, 2008
Chemical	Acid Catalysts	Medium	Medium	High	Medium	Medium	A.T.W.M. Hendriks, 2008
	Alkaline Catalysts	Good	Medium	Medium	Medium	Medium	A.T.W.M. Hendriks, 2008
	Oxidative Catalysts	Good	Good	High	Low	Good	M.J. Taherzadeh, 2008, A.T.W.M. Hendriks, 2008
Bio.	Biological	Good	Good	Medium	Low	Medium	M.J. Taherzadeh, 2008

Table 4-2: Pretreatment technologies evaluation for the biochemical plant (M.J. Taherzadeh 2008, A.T.W.M. Hendrix 2008).

Figure 7: Effect of various pre-treatment methods [58]

Regarding the power input required for grinding the particle (P_{grind}), we used in our model a simple comminution correlation provided by Miao *et al.* [59]:

$$P_{\text{grind}} = \dot{m}_{\text{BM}} \frac{\alpha}{d_p^{\beta}}, \tag{15}$$

where d_p is the characteristic size of the particle, $\dot{m}_{\text{BM}}$ is the mass flow rate of the biomass, and α and β are correlation constants. We acknowledge that our comminution model is likely to be oversimplified, as it does not account for the effect of moisture content on the required grinding energy of biomass. However, a more elaborate model for the grinding process should be considered for future work.

5.2.2 Post-Digestion Gas Conditioning

Biogas conditioning process is a necessary step after biodigestion as the gas often contains traces of undesired toxic and corrosive material like hydrogen sulfide or simply water. Biogas upgrading can be done through reaching a mixture with mainly methane (non-upgraded biogas will contain 50% to 60% methane by volume) by separating the CO_2 or by applying methane reforming reactions

for example, which is the conversion of methane to carbon monoxide and hydrogen (syngas) by the addition of steam.

The removal of unwanted contaminants from the biogas can be done using different technologies. All these can be categorized as following: Absorption, adsorption, permeation and cryogenic. The most applied technologies in anaerobic digestion and gasification systems are scrubbing, physical and chemical absorption [58]. In our model, traces of hydrogen sulfide must be separated. For the power input P_{scrub} required for gas scrubbing, we estimated the minimum work of separation as:

$$P_{\text{scrub}} = -\dot{n}RT\big(X \ln X + (1-X)\ln(1-X)\big), \tag{16}$$

where X denotes the mole fraction of the species to be scrubbed in the overall gas phase, and $\dot{n}$ is the mole flow rate of the gas phase. In reality this minimum work is not achievable and we assumed a second law efficiency $\eta_{II} = 20\%$.

5.2.3 Biodigestion Method

For this project, we choose the most mature, proven and low cost methods since the goal is to assess the feasibility of a biogas plant in Nigeria today. We choose wet fermentation in the vertical continuously stirred tank fermenter (stirring energy not modeled) as it is the most conventional reactor set-up used for wet fermentation (implemented in Germany in approximately 90% of its modern biogas plants), despite some recently highlighted limitations including difficulty in achieving complete mixing, high energy requirements associated with mixing, and disruption of microbial consortia by mixing (other methods include plug flow reactors and batch reactors).

There are several methods of anaerobic digestion, but for food waste, studies have shown that mesophilic is the most stable. Thermophilic digestion allows for faster methane extraction and therefore has a lower substrate retention time and can be considered in situations where size is a restriction, but has been shown not to be as stable and more sensitive to input composition when dealing with food waste [60].

In order to estimate the biogas yield for food waste, four different methods are usually undertaken:

1. If the ultimate analysis of the feedstock is available, a global reaction (Buswell Equation (1952)) can be used to find the final composition of the biogas. Since only a portion of the biomass can be broken down, a biodigestion efficiency has to be assumed in order to estimate the biogas yield.

2. In some cases, the exact atomic composition of the feedstock is not known and only the breakdown in term of carbohydrates, fats and proteins is known. These are usually difficult to measure for highly heterogeneous waste like organic food waste. Assumptions on an average chemical formula for different components lead in turn to estimate yields and compositions, when assuming a biodigestion efficiency that can be different for carbohydrates, protein and lipids.

3. Advanced mathematical and chemical models to predict yields and compositions of the biogas produced exist. The most advanced and commonly referred to is the Anaerobic Digestion Model 1 or ADM1. ADM1 is based on differential and algebraic equations governing the biochemical kinetic processes. The use of advanced model like ADM1 requires an extensive and precise knowledge of the anaerobic digestion biochemistry and models separately the four phases of the process: hydrolysis, acidogenesis, acetogenesis and finally methanogenesis.

4. One can build correlations for biodigestion yield and compositions based on available experimental data. However, for the specific case of food waste, the composition of the feedstock may vary considerably from a region to another, or even from a household to another within

the same area. The use of this method could be used as a way to check order of magnitudes of obtained yields.

In this project, we chose to proceed using a combination of the first and fourth methods for biodigestion yield and composition estimation. We first used published ultimate analysis for food waste in Lagos **??** to find the composition and yield. This was compared to a basket of different biomass sources likely to be part of residential food waste. Statistics obtained using this basket is used for a sensitivity analysis. The values obtained are cross-checked against experimental data gathered from literature for organic food waste.

5.3 Diesel Engine Modeling

5.3.1 Diesel Engine Retrofit

Gaseous fuel can be used in both spark ignition (SI) and compression ignition (CI) engines with appropriate relatively simple conversion [61]. In an SI engine one can operate on 100 per cent biogas or syngas, since the spark ignites the gaseous fuel/air mixture. However in a diesel engine, the gaseous fuels usually have a large octane numbers compared to conventional liquid fuels, and therefore, a high resistance to auto-igniting and knocking, hence suitable for engines with relatively high compression ratio. Since the gaseous fuel will hardly auto-ignite, a pilot diesel injection is required (between 10% and 20% depending on the load) acting as an ignition energy source. Usually dual-fuel (gaseous fuel and diesel) engines have the gaseous fuel mixed with the air in the engine cylinders, either through direct mixing in the intake manifold with air or through injection directly into the cylinder. The resulting mixture after compression is then ignited through the injection of a small amount of diesel fuel (the pilot) in the usual way. Using gaseous fuels in a dual mode diesel engine can be done without significant efficiency drop. In some instances improvements in both work output and efficiency have been reported [62].

In the case of biogas and syngas, outputs of biodigestion and gasification respectively, the gaseous fuel added to the diesel has a lower heating value per unit mass compared to pure methane due in the first case to the large amount of CO_2 and in the second case to the present of CO in the syngas, fuel which is already partially oxidized, hence its lower heating value per unit mass.

5.3.2 Flowsheet

For the modeling purpose, we assumed an idealized diesel cycle consisting of an isentropic compression, followed by isobaric combustion, isentropic expansion, and finally isochoric exhaust. The compression ratio of the diesel engine V_1/V_2 is assumed to be 20, which is within the nominal design range. We first note that the isobaric combustion is a conservative estimation. In reality, we expect the pressure to rise in the combustion chamber (as the volume also expands). Then due to the higher pressure, there will be more work that can be extracted during the expansion stroke of the engine. However, modeling the relationship between pressure and volume during the combustion process in ASPEN Plus is non-trivial, so here within the scope of this project, we simply take the conservative estimate but note that in reality, the amount of work can be increased.

We also note that there are two possible modes of running a diesel cycle. The first mode, which is common for liquid diesel, is to first compress the air only, and then inject liquid diesel droplets after the compression stroke, so that the fuel auto-ignites due to the heat. Then both the air and fuel expand and are exhausted. The second mode, which is more common for gaseous fuels, is to pre-mix air and fuel before the compression, and go through the whole cycle without adding additional fuels to the engine.

In the ASPEN Plus flowsheet, we will simulate both modes of operation, as shown in Fig. 8. However, for the base case simulation, we will choose the first mode of operation (inject fuel after

compression) due to two reasons. Firstly, in the current Lagos community, there are already operational diesel engines, which run on diesel (and thus inject the fuel after the compression stroke). The point of the biodigestion/gasification intervention is to provide an alternative energy source without needing to extensively retrofit the current diesel engine design. If we change the way the fuel is injected into the engine, this may necessitate additional investment, so before we propose this change, we want to compare the performance of the two modes of operation first. Secondly, with both biogas and syngas, it will be necessary to mix the fuel with about 10% diesel in order to ignite the mixture. However, as we are primarily interested in modeling the energy balance from the gasification and biodigestion processes, we do not account for this 10% diesel in our flowsheet energy balance.

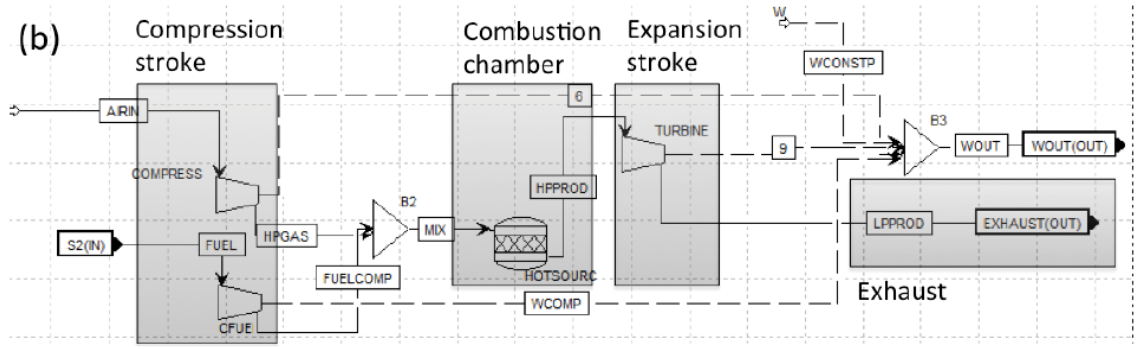

Figure 8: Flowsheet modeling of the diesel engine

5.4 System Modeling

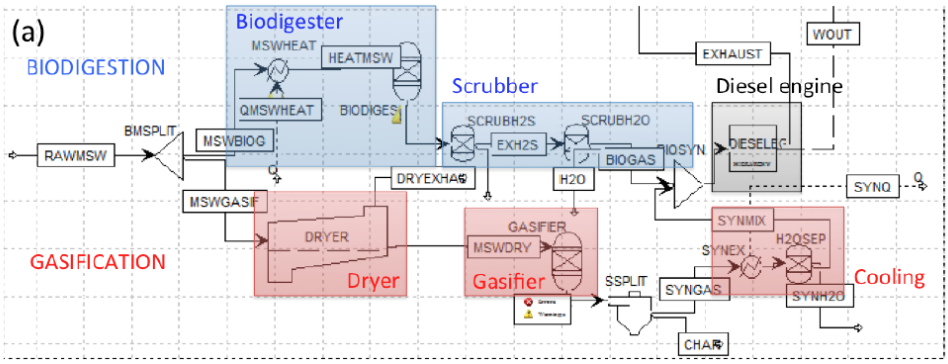

Figure 9: Flowsheet modeling of the biodigestion system (blue) and gasification system (red) in ASPEN Plus.

In order to interrogate the relative performance of gasification and biodigestion of municipal waste from the systems perspective, it is necessary for us to construct a flowsheet model to understand the overall energy balance and efficiencies. As shown in Fig. 9, the biodigestion system is modeled as a series of biodigester, scrubbing mechanism, and diesel engine. Likewise, the gasification system is modeled as a series of dryer, gasifier, and cooling components. Not shown in the flowsheet are energy calculations related to preparing and grinding the biomass to the suitable size for either process. Once syngas or biogas is produced, this fuel is then fed into the diesel engine, which is a sub-model of the system flowsheet.

6 Results: Process Modeling

6.1 Gasification Process Results

6.1.1 Base Case Results

First we establish the results for the base case scenario. In this scenario, to simplify the problem, we assume that the temperature profile along the length of the reactor is known. In the drying/pyrolysis zone (0.6 m), the temperature is assumed to be held constant at 400°C whilst solid-phase devolatilization takes place. Fig. 10 shows the solid-phase devolatilization process as a function of the reactor length, in the initial drying/pyrolysis zone at the top of the gasifier. In the different panels of the figure, we plot the different quantities such as the intra-particle temperature, moisture content, total devolatilized gas yield, and the yields of some important gas species. The different lines show the profiles at different points inside the particle: at the core, 2.5 mm from the core, and at the surface (5 mm).

As shown in all panels, there is delayed drying and devolatilization at the particle core, which is expected due to the fact that the thermally thick nature of the biomass particles will require time for heat transfer into the solid. This timescale is around a few minutes, or in terms of the reactor length, 5 cm (about 5% of the total length), which is relatively minor compared to the total residence time (hours) of the solid phase in the reactor.

Furthermore, panels (d) through (f) show the dynamics of the devolatilized species—CO, methanol, and carbon dioxide. We observe that while CO and CO_2 have a relatively transient devolatilization dynamics (i.e. all these species have completed devolatilization quickly), species such as methanol has a much longer timescale for devolatilization. In the Ranzi kinetic scheme, this is due to the existence of so-called "trapped species": partially devolatilized molecules which are still bound to the solid phase, but which takes a much longer timescale to be released in the gaseous phase.

At the end of the solid devolatilization phase at 400°C, we transferred all the devolatilized gas species into a new Cantera object programmed to perform the gas-phase Ranzi kinetic mechanism. We assume that the combustion zone is very thin (around 1 mm in axial thickness), the temperature of the combustion zone is constant at 1000°C, and that air (O_2 and N_2) is being supplied at an air/fuel equivalence ratio of 0.2. The injected air is designed to provide a limited extent of exothermic combustion, and the heat of reaction is used to both heat up the biomass as well as to drive the endothermic component of the gasification reaction. These assumptions are consistent with typical gasification values found in the literature and existing designs.

Fig. 11(a) illustrates the evolution of the major gaseous species (hydrogen, carbon dioxide, CO, oxygen, and methane) as a function of reactor length. As we can see, at the high temperature, the lean oxygen becomes consumed immediately, and the other species evolve in a correspondingly short timescale of around 0.3 s (or about 0.1 mm in the reactor length). Because the burning is lean, we have a preferential production of CO over CO_2, which is what we want for the ensuing syngas production.

Once combustion is complete, the next zone is the reduction zone. Here, we once again assume a known temperature profile of a steady 800°C over the whole length (0.3 m). In the reaction zone, two types of reactions will occur: the homogeneous gas-phase reactions, as well as the heterogeneous char-gas reactions. While the Ranzi mechanism gives a detailed account for both, it is unfortunate that we were unable to adapt the heterogeneous char-gas reaction kinetics into Cantera object, because as shown in Table 4 previously, the char reaction rates have fractional power dependencies on the gaseous species, and in Cantera there is no feasible way to specify these fraction power coefficients. Instead, we first completely ignore the heterogeneous reactions, and focus our attention on the gas-phase reactions first.

Fig. 11(a) illustrates the time evolution of the major gas species (hydrogen, carbon dioxide, CO, oxygen, and methane) inside the reduction zone due to the Ranzi gas-phase reactions only. We see

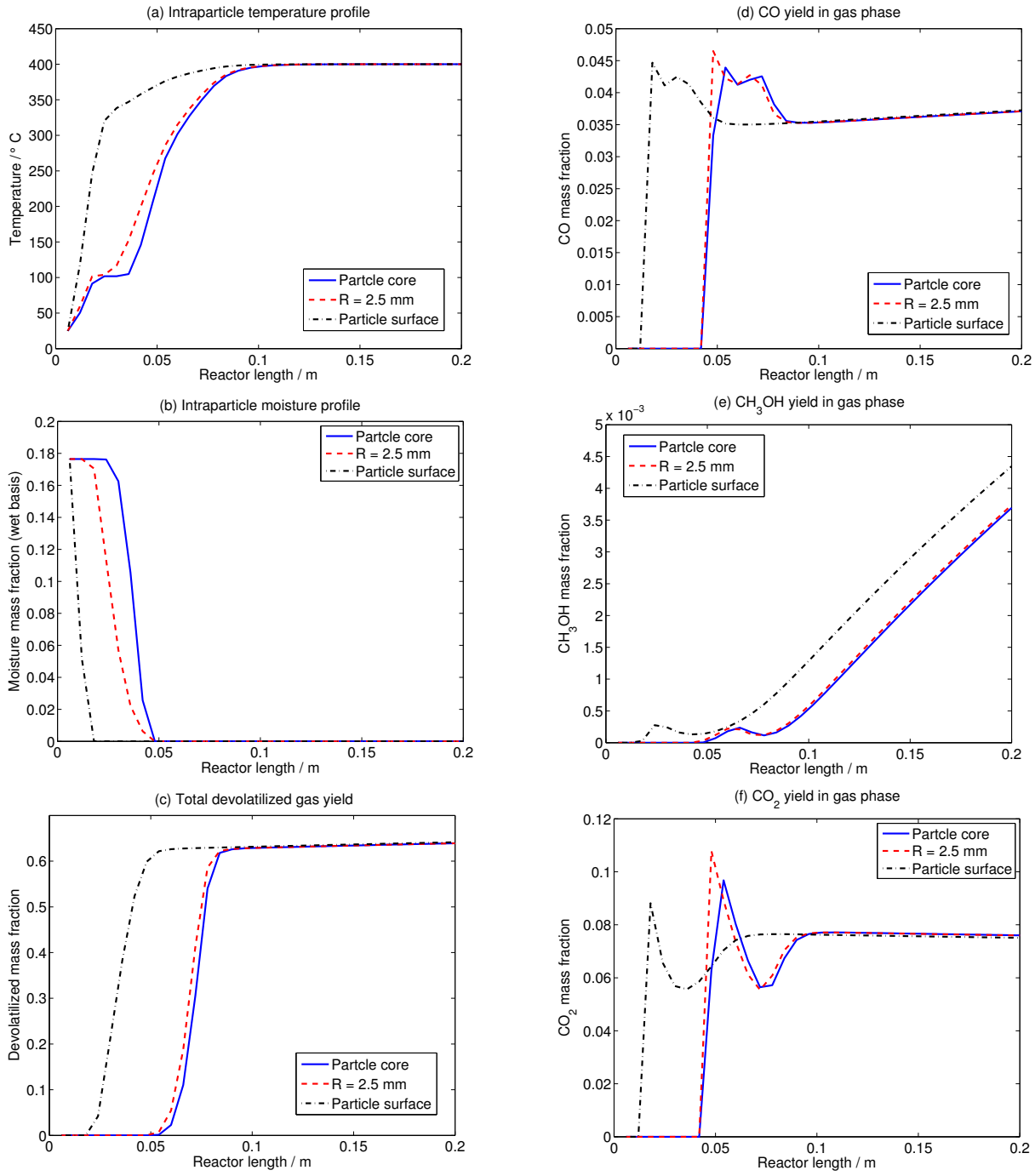

Figure 10: Simulation results of solid-phase devolatilization from 10-cm-diameter single-particle model based on the Ranzi pyrolysis kinetics [48], as a function of reactor length. (a) Intra-particle temperature profile, (b) intra-particle moisture profile, (c) total devolatilized gas yield, (d) CO yield in the gas phase, (e) methanol yield in the gas phase, and (f) carbon dioxide yield in the gas phase. The blue solid lines denote profiles at the particle center; red dashed lines, at a distance 2.5 cm from the center; and black dash-dotted lines, at the particle surface (5 cm from the center).

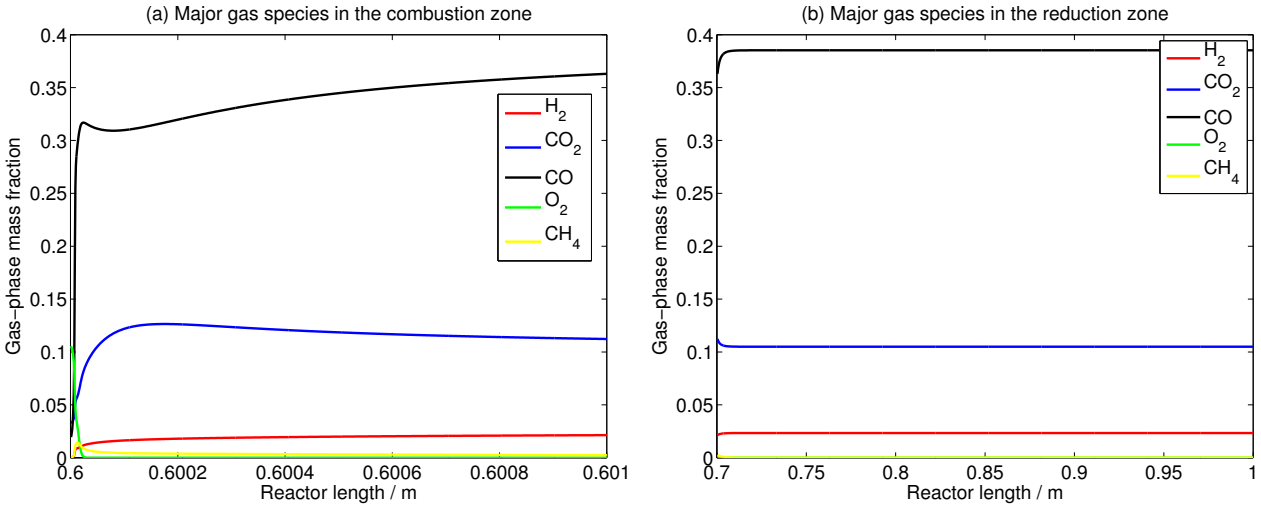

Figure 11: Simulation results of gas-phase reactions based on the Ranzi kinetics scheme [48], as a function of reactor length. (a) Major gas species inside the combustion zone, and (b) major gas species inside the reduction zone, before accounting for heterogeneous char reactions. The equivalence air/fuel ratio is set to 0.2 at the beginning of the combustion zone.

that, in the absence of oxygen, very little is happening to the species: barring from the initial transient change in the species concentrations (presumably due largely to the changed temperature and thus equilibrium), for the remaining part of the reduction zone, the relative abundance of these major gas species remains more or less constant.

This observation does somewhat simplify the problem of the heterogeneous char-gas reactions for us. If it is true that not much is happening in the gas phase, perhaps we can reasonably decouple the homogeneous gas-phase reactions from the heterogeneous reactions (with some caveats to be described later).

For the heterogeneous reactions, we have three competing char reactions. Based on the flow rate of the gas phase and the approximate residence time, we first calculated the effective molar concentrations of the relevant gas species based on the results from the gas phase reactions: $[O_2] \approx 1.9 \times 10^{-11}$ kmol/m^3, $[H_2] \approx 2.6 \times 10^{-3}$ kmol/m^3, $[H_2O] \approx 2.0 \times 10^{-3}$ kmol/m^3, $[CO] \approx 3.1 \times 10^{-3}$ kmol/m^3, and $[CO_2] \approx 6.2 \times 10^{-4}$ kmol/m^3. To estimate the effective concentration of char, we take the known mass flow rate of char, multiplied by the carbon elemental composition (around 60%), and adjusted properly for the solid-phase residence time, which is known. This gave us an approximation of [Char] ≈ 14 kmol/m^3. So as we can see, char is in great excess compared to the other gaseous species. So for the reactions described in Table 4, we simply assume that all the reactions are zeroth order with respect to char, and set [Char] ≈ 1.

This simplification effectively reduces our rate equations to the following type:

$$\frac{d[X]}{dt} = -k[X]^\gamma, \text{and} \tag{17}$$

$$\frac{d[Y]}{dt} = k[X]^\gamma. \tag{18}$$

where $[X]$ refers to the concentration of the relevant gaseous species, and $[Y]$ refers to a product as a result of the consumption of X. This system of equations actually has an analytical solution. For the first differential equation, integrating both sides and setting the initial condition $[X](t=0) = [X]_0$, we arrive at the following implicit expression:

$$\frac{1}{1-\gamma}\left([X]^{1-\gamma} - [X]_0^{1-\gamma}\right) = -kt, \gamma \neq 1. \tag{19}$$

Given a pre-calculated gas-phase residence time $\tau_{\text{res,gas}} = \rho_{\text{gas}} A_{\text{react}} L_{\text{red}} / \dot{m}_{\text{gas}}$, we can analytically solve for the final species concentration:

$$[X] = \left([X]_0^{1-\gamma} - (1-\gamma) k \tau_{\text{res}} \right)^{\frac{1}{1-\gamma}}. \tag{20}$$

Plugging this into the second differential equation, we obtain:

$$\frac{d[Y]}{dt} = k \left([X]_0^{1-\gamma} - (1-\gamma) k t \right)^{\frac{\gamma}{1-\gamma}}. \tag{21}$$

Integrating both sides and setting the initial condition $[Y](t=0) = [Y]_0$, we obtain:

$$[Y] = [X]_0 + [Y]_0 - \left([X]_0^{1-\gamma} - (1-\gamma) k \tau_{\text{res}} \right)^{\frac{1}{1-\gamma}}. \tag{22}$$

Now, in the context of our heterogeneous char-gas reactions, we calculated the following rate constants and initial reaction rates (using the estimated effective concentrations of the gaseous species listed previously) at 800°C in Table 6.

Table 6: Heterogeneous char-gas reaction kinetic scheme, from [48]

Reactions	Rate constant	Overall reaction rate
Char + $O_2 \rightarrow CO_2$	3170	6.0×10^{-8} kmol/s
Char + 0.5 $O_2 \rightarrow$ CO	4150	1.8×10^{-5} kmol/s
Char + $H_2O \rightarrow$ CO + H_2	0.643	8.4×10^{-4} kmol/s

From Table 6, we see that while the char-water reaction has a low rate constant, the relative abundance of water actually makes the overall reaction rate the fastest of the three. Because oxygen in the reduction zone is very lean and decreasing, and because the first CO_2-producing reaction has an overall reaction rate that is one-thousandth of those of the other two reactions, we can safely ignore the CO_2-producing reaction in the reduction zone, and focus our attention on the reactions producing CO and H_2.

For the different species, according to the analytical solution above, we have the following time evolution:

$$[\text{H}_2\text{O}](t) = \left([\text{H}_2\text{O}]_0^{0.3} - 0.3 k_3 t \right)^{\frac{1}{0.3}}, \tag{23}$$

$$[\text{O}_2](t) = \left([\text{O}_2]_0^{0.22} - 0.11 k_2 t \right)^{\frac{1}{0.22}}, \tag{24}$$

$$[\text{H}_2](t) = [\text{H}_2]_0 + [\text{H}_2\text{O}]_0 - \left([\text{H}_2\text{O}]_0^{0.3} - 0.3 k_3 t \right)^{\frac{1}{0.3}}, \text{and} \tag{25}$$

$$[\text{CO}](t) = [\text{CO}]_0 + [\text{H}_2\text{O}]_0 + [\text{O}_2]_0 - \left([\text{H}_2\text{O}]_0^{0.3} - 0.3 k_3 t \right)^{\frac{1}{0.3}} - \frac{0.22}{0.11} \left([\text{O}_2]_0^{0.22} - 0.11 k_2 t \right)^{\frac{1}{0.22}}. \tag{26}$$

This set of equations can be plotted analytically for the length of the reactor, as seen in Fig. 12. As expected, as the reduction zone progresses, water is consumed (it should be noted that much of this water comes from the drying process), and the production of syngas (CO and H_2) increases, as what gasification should be.

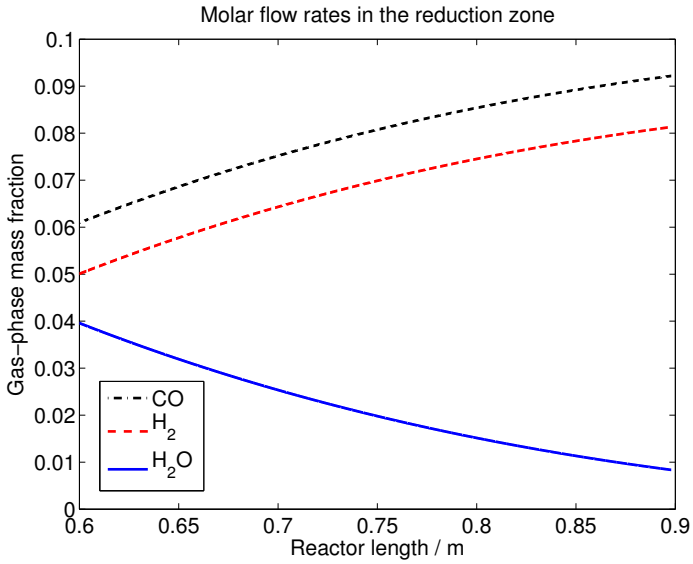

Figure 12: Evolution of the major gas species due to heterogeneous char reactions in the reduction zone of the gasifier. Blue solid line: CO; red dashed line: hydrogen gas; black dash-dotted line: water vapor. The species evolve at 800°C.

Of course, our assumption of decoupling the gas-phase from the heterogeneous reactions is not completely valid, as it is well known that the consumption of water and the production of CO, H_2 and CO_2 will affect the equilibrium balance of the water-gas shift reaction (which is described in the Ranzi gas phase mechanism). In fact, had we accounted for the water-gas shift reaction, we would expect that due to decreasing water concentration, the equilibrium will favor the formation of more CO and water. We acknowledge this error, but will leave further quantification of the water-gas shift reaction to future studies.

Table 7: Major Species at the Outlet of the Gasifier, at 800°C

Species	Molar flow rate (mol s^{-1})	Mole fraction	Experimental (Arnavat [51])
CO	0.0922	0.364	0.17-0.22
H_2	0.0813	0.321	0.12-0.20
N_2	0.0571	0.225	0.50-0.54
CO_2	0.0121	0.048	0.09-0.15
H_2O	0.0084	0.033	-
C_2H_2	0.0013	0.005	-
CH_4	7.9782×10^{-4}	0.003	0.02-0.03
H	3.7357×10^{-5}	-	-
CH_3	1.4837×10^{-5}	-	-
C_2H_4	1.4201×10^{-5}	-	-
C(char)	0.0483		

At the outlet, we have the following major species shown in Table 7.1, and compare the mole fractions with an experimentally obtained dataset for woody biomass. As we can see, while the relative CO/H_2 fraction is within the range, the mole fractions of CO and H_2 seem over-estimated, while the mole fractions of N_2, CO_2, and CH_4, under-estimated. One potential reason for underestimating nitrogen/carbon monoxide and overestimating syngas is that we are using much less air in the process. For example, while the air/fuel equivalence ratio used in our model is 0.2, the Arnavat study used ratios ranging from 0.25 to 0.47 [51]. While we could have adjusted our Cantera parameters to

more closely resemble the Arnavat study, there are specific reasons why we decided not to do so, as will be discussed later in the technical constraints in running a diesel cycle on syngas. Also, while Arnavat used primarily woody biomass in the gasification experiments, we used data from municipal solid waste, which will have a different elemental composition and biomass structure, thereby giving different relative yields. Finally, the underestimation of CH_4 is likely due to ignoring the steam reformation reaction due to the way we modeled the gas-phase and heterogeneous reactions independently, the same way as we ignored the water-gas shift reaction.

6.1.2 Sensitivity of the Gasification Process on Biomass Types

One of our main motivations for developing a detailed chemical kinetics and reactor model for gasification is that it will enable us to assess the sensitivity of gasification outputs as a function of the variation in the inputs. As we know, different types of biomass have different ultimate/proximate analysis values, as well as lignin-cellulose-hemicellulose contents. The Ranzi kinetic mechanism has been shown previously (in Kevin Kung's thesis research) to be generalizable to a diverse range of biomass types (with reasonable match to a variety of experimental data), insofar that the appropriate input biomass characterization parameters be known accurately.

Given that the municipal solid waste is a composite of many different types of wastes, and its composition may fluctuate from day to day and season to season dependent upon what types of biomass is discarded int he neighborhood, we find it appropriate to undertake an investigation of how sensitive the gasifier output will be to such variations in the input feedstock.

In order to do so, we compiled a database of more than 200 biomass types from a diverse range of literature sources. We selected 15 biomass types where both the ultimate analysis and the lignin-cellulose-hemicellulose compositions are well known. These biomass types are: almond, bamboo, barley straw, beech wood, corncob, corn stover, eucalyptus, hazelnut, olive husk, poplar, sugarcane bagasse, switchgrass, tea waste, tobacco leaf, and wheat straw. We ran these different types of biomass under the same Ranzi kinetic mechanism and gasifier conditions as described in the base case above. Fig. 13 illustrates the solid-phase devolatilization dynamics as a function of the reactor length, and each different biomass type is shown as a line of different color and line style.

As observed, panels (a) and (b), which correspondingly show the temperature profile and the moisture content, have very little variation as a function of the different types of biomass. Panel (c), which shows the total devolatilized gas mass fraction evolution, has a comparably wider spread, reaching a range of around 25%. In contrast, panels (d), (e), and (f)—which illustrate the devolatilization of specific gas species—show a much more significant variation for different types of biomass. This trend may at first seem disheartening, as the gasifier performance seems to vary drastically depending on the biomass input. However, we need to examine further into how these different volatile gases react in the ensuing combustion/reduction zones before arriving at a conclusive answer.

Fig. 14 shows the evolution of major gas species in the combustion zone of the gasifier, for four different types of biomass: almond, bamboo, sugarcane bagasse, and tea waste. Perhaps a bit surprisingly, we see that despite the wide variation in the solid-phase devolatilization as noted earlier, once we reach the combustion zone, all the devolatilized species seem to react with oxygen and give a relatively consistent output from biomass to biomass, with an error range of 3%. Therefore, we came to the conclusion that despite the wide biomass-dependent variations in the different devolatilized gas species as observed in panels (d), (e), and (f) of Fig. 13, these variations tend to disappear. The only biomass-dependent variation in Fig. 13 that we should be concerned about is illustrated in panel (c), where the different types of biomass may give rise to different mass yield of gas. This will affect the mass flow of the syngas in the final system per unit mass flow of biomass, and will therefore affect the overall system performance.

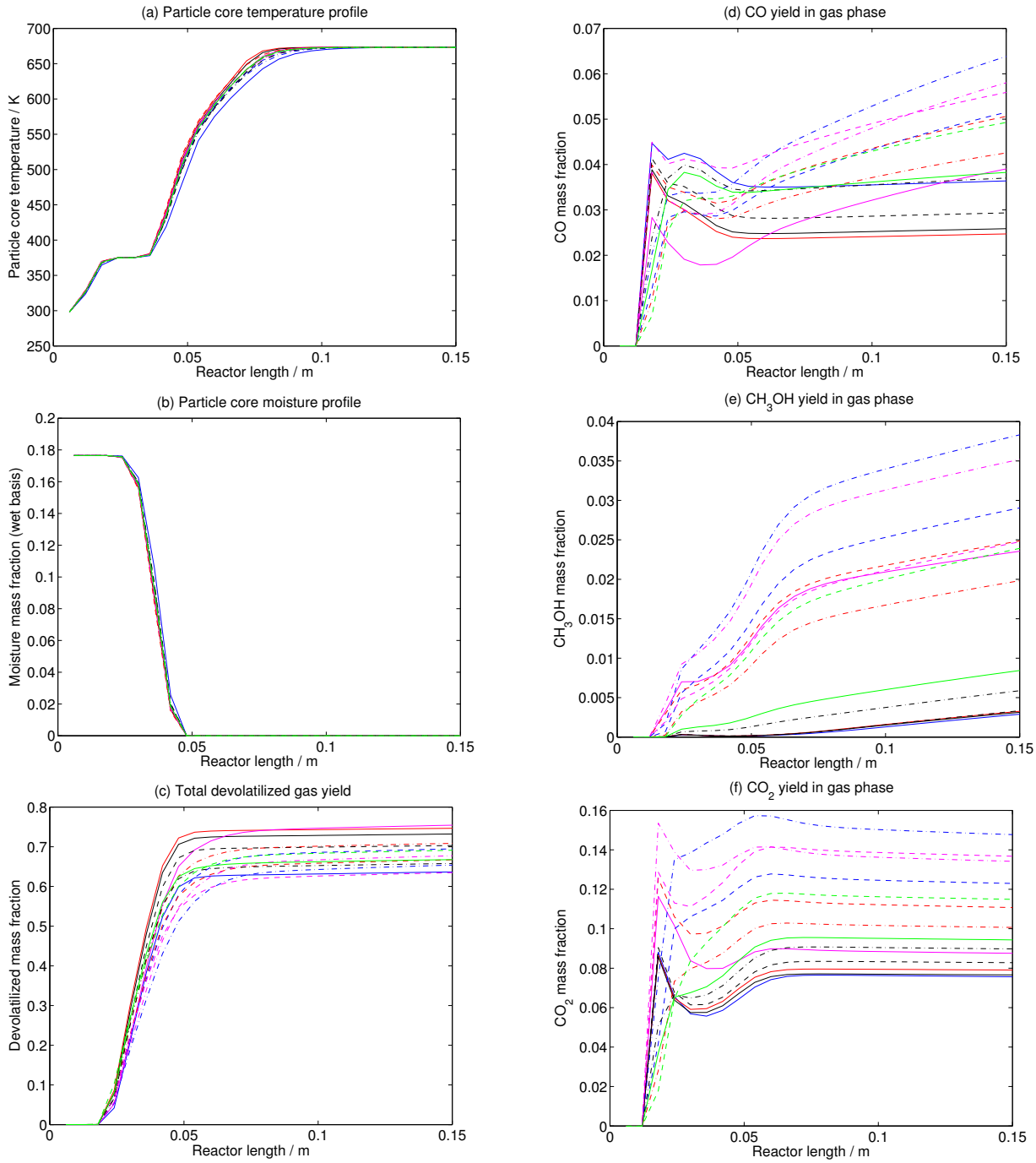

Figure 13: Simulation results of solid-phase devolatilization from single-particle model based on the Ranzi pyrolysis kinetics [48] for different types of biomass, as a function of reactor length. (a) Intra-particle temperature profile, (b) intra-particle moisture profile, (c) total devolatilized gas yield, (d) CO yield in the gas phase, (e) methanol yield in the gas phase, and (f) carbon dioxide yield in the gas phase. The different lines of different styles denote the different types of biomass.

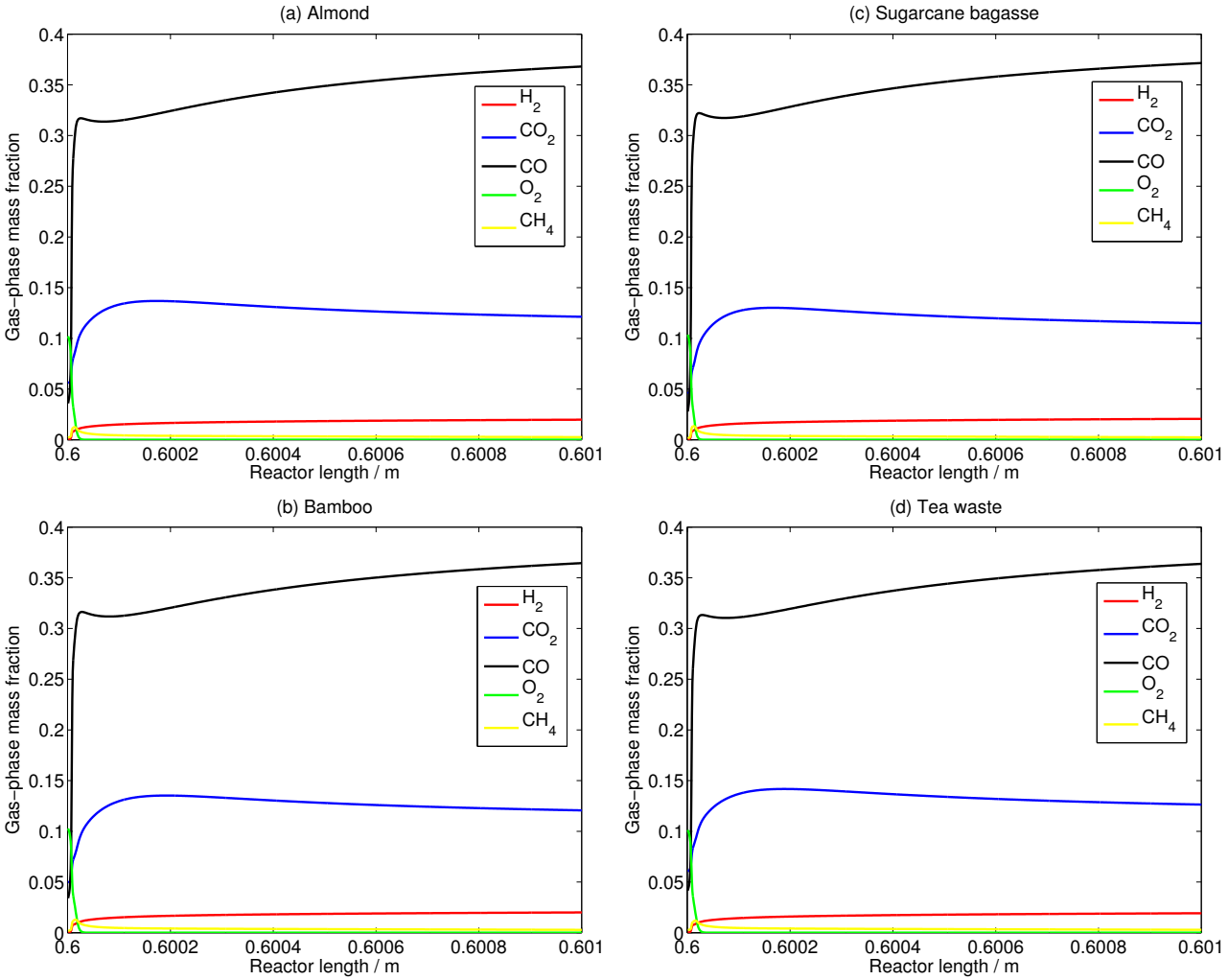

Figure 14: Simulation results of gas-phase reactions based on the Ranzi kinetics scheme [48], for different types of biomass, as a function of reactor length. (a) Almond, (b) sugarcane bagasse, (c) bamboo, and (d) tea waste. The equivalence air/fuel ratio is set to 0.2 at the beginning of the combustion zone.

6.2 Biodigestion Process Modeling Results

We first estimate the chemical formula of the food waste from Lagos **??**:

Table 8: Estimated MSW Composition for Lagos

Atom	Weight%	Adjusted Weight%	Mole%	Molar Mass (g/mol)
C	51.33	55.93	32.59	12
H	6.77	7.37	51.59	1
O	30.92	33.69	14.73	16
N	1.42	1.54	0.772	14
S	1.34	1.46	0.319	32

We obtain the following chemical formula for our feedstock:

$$C_{102.1}H_{161.7}O_{46.17}N_{2.4}S_1$$

Using the following global reaction for anaerobic biodigestion **Buswell Equation (1952):**

$$C_cH_hO_oN_nS_s + \frac{4c-h-2o+3n+2s}{4}H_2O \rightarrow \frac{4c-h+2o+3n+2s}{8}CO_2 + \frac{4c+h-2o-3n-2s}{8}CH_4 + nNH_3 + sH_2S$$

The global biodigestion reaction becomes:

$$C_{102.1}H_{161.7}O_{46.17}N_{2.4}S_1 + 40.89\ H_2O \rightarrow 43.53\ CO_2 + 58.57\ CH_4 + 2.4\ NH_3 + \ H_2S$$

This leads to the following final composition of the biogas:

Table 9: Estimated biogas composition for Lagos (Molar%)

Product	Mole%
CO_2	41.26
CH_4	55.52
NH_3	2.275
H_2S	0.947

The analysis based on the Buswell equation gives us the composition of the biogas but assumes complete biodigestion of the food waste, hence over estimate the biogas output per ton (dry) biomass used. In reality, only a percentage is biodigested, this percentage depending on hardly biodigestable materials typically lignin. For food waste, realistically 40% to 65% of the initial biomass is broken down into biogas [**?**]. A value of 65% would be reached for food scraps with relatively lower lignin and hemicellulose or after an effective pre-treatment step. Based on this more realistic range of conversion of 40% to 65%, the biodigester output per unit dry mass of biomass is estimated within the range [461-749] m^3 per ton of volatile solid (VS). The biogas obtained has a heating value of approximately 18 MJ per m^3 once trace components removed.

In order to check the validity of the obtained biodigestion yield, a comparison with reported experimental results is needed. Curry [**?**] reports a mesophilic biodigestion yield for food waste of 367 m^3 per ton of volatile solid basis. In figure 15, different feedstock biomass are shown along with their biodigestion yields [**?**]. Assuming organic food waste to be an average of all these experimental values, we obtain experimental biogas yield in the range [342-407] m^3 per ton biomass (VS).

Source	Biogas yield m^3/tVS
Discarded Food	355 [34]
Food waste	367 [11]
OFMSW	310–490 [35]
OFMSW	300–400 [26]
OFMSW	255–494 [36]
Food Waste	288 [32]
OFMSW	390 [33]
Food Waste	472 [27]

Figure 15: Experimental biogas yield for food waste from different sources

The previous assessment shows that our estimate for biogas yield using Buswell equation along with a biodigestion efficiency, in the case of food waste in Lagos are realistic. Our system analysis will use a base case value of 400 m^3 per ton biomass (VS).

6.2.1 Sensitivity of the biodigestion Process on Biomass Types

The results of a sensitivity analysis of the biogas yield and composition to the biogas yield are now shown. We used a basket of biomass sources that are likely to be part of the organic food waste. These have been previously gathered in our biomass database presented in the first phase of this study (midterm report). The result of ultimate analysis for these biomass sources is known. Figure 16 shows the variations in composition and yield for the selected biomass.

	Biogas composition (%molar)				Yield (m3/ ton biomass VS)	
Lignocellulosic residues	CH4 %molar	CO2 %molar	NH3 %molar	H2S %molar	Min 40% conversion	Max 65% conversion
Almond shell	51.670	46.290	1.991	0.051	417.4	678.3
Bamboo	48.800	50.520	0.655	0.029	428.7	696.6
Barley straw	51.130	47.580	1.199	0.097	407.3	661.8
Beech bark	51.170	47.600	1.153	0.079	423.8	688.7
Corn Cob	49.010	50.290	0.695	0.000	408.2	663.3
Corn Stover	49.910	48.990	1.030	0.075	414.9	674.1
Eucalyptus	50.530	49.190	0.265	0.008	400.5	650.9
Hazelnut shell	50.530	49.190	0.265	0.008	400.5	650.9
Olive Husk	50.410	46.880	2.674	0.037	412.5	670.4
Poplar	50.470	48.700	0.825	0.008	405.8	659.4
Sugar cane bagasse	51.200	48.410	0.343	0.045	410.8	667.6
Switch grass	52.500	45.910	1.445	0.150	423.2	687.8
Tea Waste	49.190	49.880	0.885	0.046	403.7	656.0
Tobacco Leaf	50.760	47.400	1.838	0.000	420.0	682.5
Wheat Straw	50.800	47.870	1.198	0.127	407.5	662.2

Figure 16: Sensitivity Analysis of Biogas Composition and Yield

	CH4	CO2	NH3	H2S
mean	50.5	48.3	1.1	0.1
st dev (% of mean)	2.0%	2.9%	61.7%	92.5%
min	48.8	45.9	0.3	0.0
max	52.5	50.5	2.7	0.2

Figure 17: Statistics - sensitivity analysis

A low standard deviation is associated with the percentage of methane and carbon dioxide of the biogas as well with the biogas yield. For a conservative biodigestion efficiency of 40%, the average yield of 412 m^3 per ton of volatile solid (VS) is obtained with only a 2.1% deviation from the mean. The uncertainty regarding traces seems higher, especially for hydrogen sulfide. This will have an implication on the amount of work required for gas separation before using the biogas in the diesel generator.

7 Results: Diesel Engine Modeling

Here, we discuss the results related to two modes of operating the diesel engine: fuel injection after compression (base case), or fuel injection before compression, and evaluate the engine cycle efficiencies with respect to the two waste management pathways.

7.1 Mode 1 – Post-Compression Fuel Injection (Base Case)

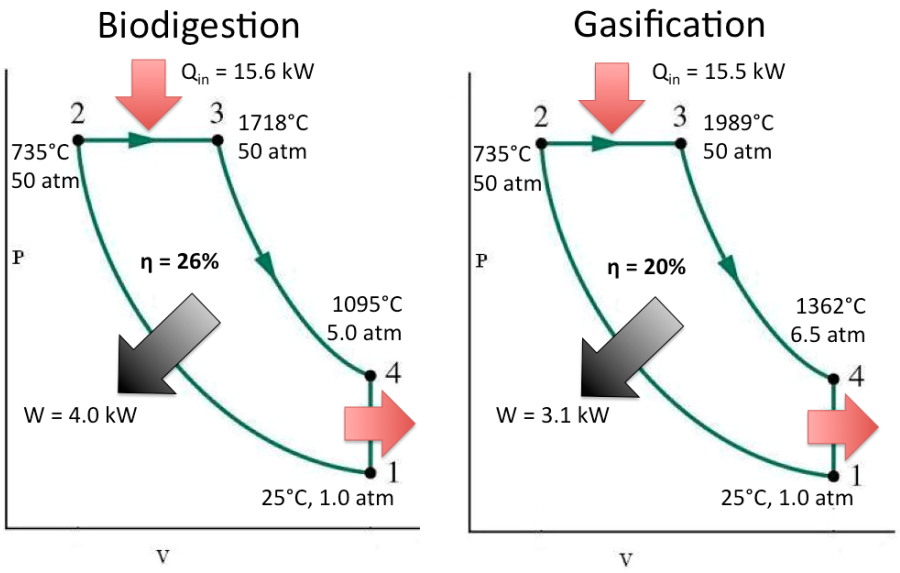

Figure 18: P-V diagrams of the diesel engine performance for biodigestion (left panel) and gasification (right panel), for the base case of fuel injection after air compression

Fig. 18 illustrates the P-V diagrams of the base cases from biodigestion (left panel) and gasification (right panel). While the initial atmospheric air starts at the same point (25°C, 1 atm) and follows the same isentropic compression path, because the differing reaction thermochemistry and fuel composition, biodigestion and gasification bring the engine to different points on the P-V diagram after the combustion chamber (point 3). This is important, as then the engine will follow different isentropic

lines as it expands from point 3 to point 4. This in turn affects the amount of work that is done, and thus the overall engine performance.

One point of caution in interpreting the P-V diagram is that points 1 and 2 show the compression of air, and at point 2 injected into the engine is fuel, which ignites spontaneously. This is how a diesel engine works in practice. Therefore, mass is not conserved throughout the P-V cycle, and the extra work needed to compress the fuel is not shown in the P-V diagrams. When we sum up all the work that is required to compress both the air and the fuel, we find that gasification, while apparently having a larger integration area under the P-V diagram, actually has less efficiency compared to biodigestion (13% versus 7.5%). There are several reasons for this. Firstly, per volume basis, methane is about 3 times as energy dense as syngas (about 800 kJ/mol versus 280 kJ/mol respectively, in terms of lower heating value). This matters because in order to achieve a similar heat of reaction, we will need to compress more volume of syngas compared to methane, and thus expend more work. Secondly, for both the oxidation of hydrogen gas and carbon monoxide, we start with 1.5 moles of reactants (for example, CO + 1/2 O_2) and end with 1 mole of product (in this case, CO_2). Whereas, in the case of methane (biogas), 3 moles of reactants (CH_4 + $2O_2$) give rise to 3 moles of products (CO_2 + $2H_2O$). This is significant, because it implies that for syngas, there are fewer moles of gas in the post-combustion products available to do the work in the expansion stroke compared to biogas. Thirdly, if we focus on the relative stoichiometry of the reactants, we realize that for every molecule of oxygen, there are 2 molecules of syngas (of either species), while there are only 0.5 molecules of methane. Given a diesel engine of a particular intake volume (of atmospheric air), more molecules of syngas needs to be compressed at each engine cycle to burn the fuel at a given air/fuel stoichiometric ratio, and this contributes towards the energy penalty for the gasification process. In contrast, in terms of biogas, per engine cycle, there are fewer molecules of biogas to compress given a fixed initial air intake volume. From the perspective of the engine, for a given mole flow rate of fuel, it is running faster for biogas than it is for syngas. Fourthly, while biogas is relatively "cold" (37°C), syngas is hot (≈ 800°C). Compressing syngas at its exit temperature from the gasifier turned out to have such a high penalty that we were forced to cool the syngas down to 90°C first before compressing it. Even so, syngas is still relatively hot compared to biogas, and it would not be surprising that, given the same moles of gas, a larger amount of work is needed to compress syngas.

In fact, this efficiency constraint of the diesel engine is one reason why we needed to keep the air/fuel equivalence ratio for the gasifier low in contrast to many current studies/designs: we want the input fuel stream into the diesel engine to have as little inert molecules as possible (such as N_2 and CO_2). As an illustration, originally, we utilized the syngas composition as given experimentally by Arnavat [51] as listed in Table . What we soon realized was that compressing a syngas stream containing about 70% v/v of inert gases is highly unfeasible: in fact, the power needed for fuel compression in this case was so high that the overall efficiency of the diesel cycle turned out to be negative. In this prohibitive scenario, one might entertain the idea of filtering out the N_2 beforehand so that only the combustible portion of the mixture goes into the diesel engine. There are two problems with this. Firstly, at the small scale of around 70 households, investing in a nitrogen-scrubbing component is quite costly. Secondly, the approximated work to remove nitrogen, according to the idealized entropy of mixing model, is on the order of:

$$P_{\text{scrub,N2}} = -2(0.25\text{mol/s})(8.314\text{J/molK})(360\text{K})(0.5\ln 0.5) \approx 0.5\text{kW}. \tag{27}$$

However, if we re-run our base case after scrubbing nitrogen gas, we found that there is a marginal increase in the work output by 0.3 kW (thereby increasing the diesel engine efficiency from 7.5% to 10%), which is on the same order as the work required to scrub the gas in the first place. Therefore, there is nothing much to be gained by removing the inert nitrogen from the syngas mix. On the other hand, if we reduce the air/fuel equivalence ratio, then we would conserve more biomass for syngas production, obtain a syngas composition of higher fuel volume fraction, and achieve a higher engine efficiency. Then, the exhaust heat from the diesel cycle can be used to supply heat to the gasifier,

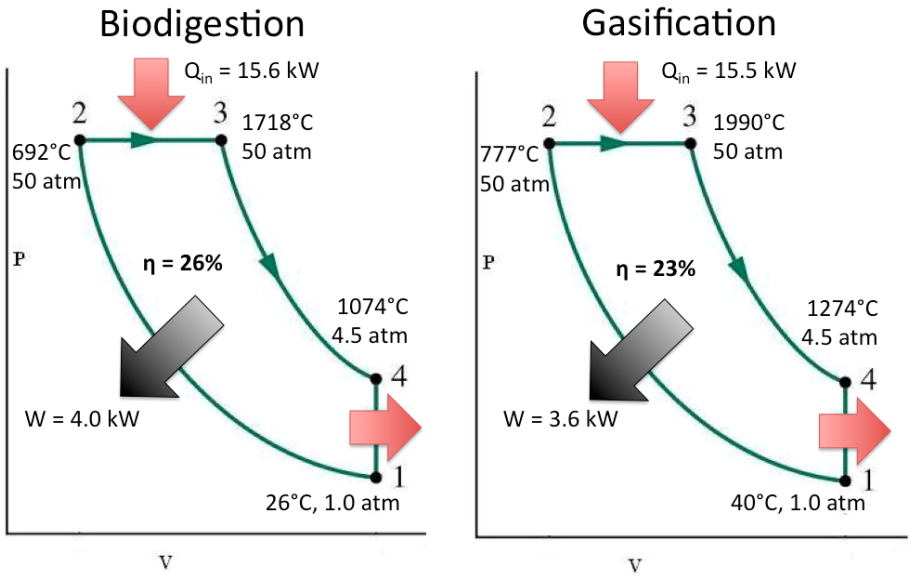

Figure 19: P-V diagrams of the diesel engine performance for biodigestion (left panel) and gasification (right panel), for the modified case of pre-mixing air and fuel before the compression stroke

in lieu of directly oxidizing biomass. This will also result in a higher overall system performance efficiency, as we will discuss next.

7.2 Mode 2 – Pre-Compression Fuel Injection

We also modified our ASPEN Plus flowsheet to consider the possibility of pre-mixing the biogas/syngas and air before the diesel compression stroke. Fig. 19 illustrates the modified engine performance. As can be noted, the efficiencies in both cases increased. In particular, there is a significant improvement in the engine efficiency when run on syngas: in fact, the two pathways now have comparable efficiencies of around 14-15%. One key reason for this improvement, if we compare Fig. 18 and Fig. 19, is that in the base case, points 1 and 2 for both syngas and biogas are at the same P-V states: 25°C and 1 atm for point 1 and 808°C and 50 atm for point 2. This is expected as in the base case, the compression cycle only starts with air, and the compression ratio is the same in both cases. In contrast, for mode 2, we note that at point 1, the fuel/air mixture already starts at different points on the P-V diagram: the syngas/air mixture, for example, has a higher initial temperature (40°C) because it enters into the engine hotter than biogas. In the rest of the processes, syngas has a consistently higher temperature (which meant less volume at the same pressure) compared to biogas. While more work is required to compress hot gas, even more work can be extracted from the hotter expanding post-combustion gas. This compensates for the various energy penalties for the syngas cycle mentioned previously.

Therefore, from these comparative studies, we can draw the conclusion that, if gasification were to be implemented, if the cost of retrofitting the diesel engine to pre-mix gas and fuel is not a concern, then doing so would significantly add to the efficiency of the diesel cycle.

8 Results: System Modeling

In order to meaningfully compare the two separate biomass treatment pathways, we need to define a ”common denominator” that allows us to define the overall system efficiency. This is done using the calorific value of the Lagos municipal waste, which was found to be 7.6 MJ/kg (wet basis) [63].

Assuming the base case flow rate specified previously (119.7 kg/day at 49.9% moisture content), this corresponds to 31.9 kW. It is expected that in the ensuing energy conversion processes of biodigestion or gasification, some fraction of this 31.9 kW will be lost. The overall system efficiency will be inferred based on how much of this original energy is lost.

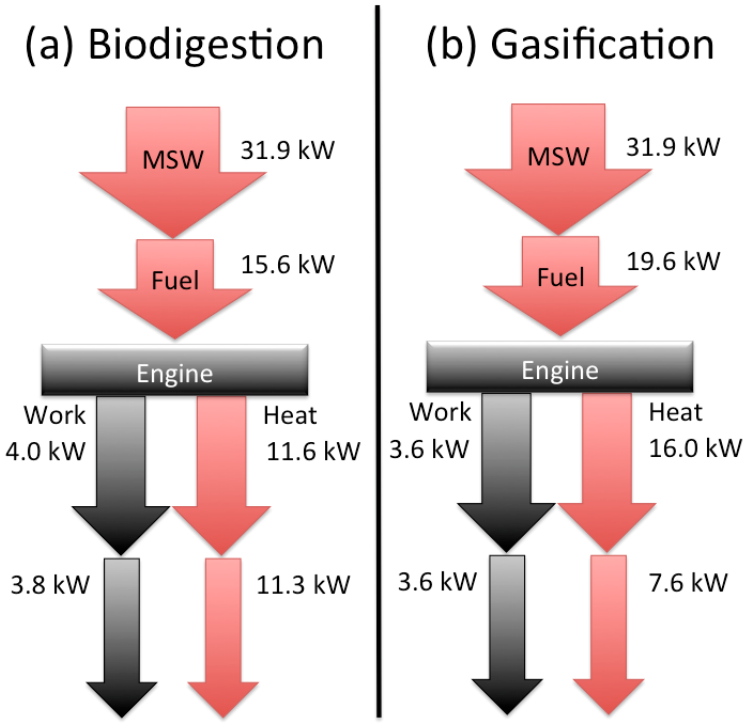

Figure 20: The overall system energy balance for (a) biodigestion, and (b) gasification.

First, we quantify the system performance of the chemical reactor by asking the following question: of the 31.9 kW of biomass input, how much of this is converted into usable fuel (syngas or biogas)? Fig. 20 shows the overall outcome for both biodigestion and gasification. For either process, there are conversion losses. For the case of biodigestion, we know, for example, that the digestion of organic waste is never complete, and there is always effluent organic content. For the case of gasification, the input of air to combust the biomass, which provides heat for the gasification system, also subtracts energy away from the overall biomass. As we can see, while for biodigestion about 49% of the MSW heating value is converted into fuel, for gasification, this figure is higher at about 62%. One caution is that there is no obvious basis to compare the heating values of syngas versus biogas at this stage, because these two fuels emerge from the reactor at different temperatures. For example, syngas in appearance carries more energy because it is at 800°C—and in fact, in the ASPEN Plus flowsheet, we actually extracted some heat when we cool the syngas down before compressing it in the diesel engine. In fact, if we com are the higher heating value of syngas and biogas at about room temperature, they are roughly equivalent (as seen in Fig. 19 previously, syngas has a Q_{in} of 15.5 kW into the engine, while biogas, 15.6 kW). In fact, some heat or work from downstream will need to be re-diverted back into the reactor to produce these gases in the first place.

After the diesel engine, we observe that the biodigestion stream has slightly higher work output (at 4.0 kW) compared to syngas (3.6 kW). However, the work that needs to be re-directed back to the previous fuel processing steps is also higher for syngas, one key reason being that it is necessary to scrub hydrogen sulfide (H_2S) before the gas enters into the engine. The various scrubbing and grinding energies add up to about 4% of the total work output. On the other hand, there is a lighter "tax" on the power output from gasification: it is less than 1%, and mainly relates to blower in the downdraft gasifier.

Another interesting observation is that, while syngas on appearance has more conversion efficiency from the gasifier, some of this energy is in term of the lower-quality heat (at 800°C) which does not make its way into the work stream, but rather, the exhaust heat stream from the diesel engine. This is corroborated by the observation, in Fig. 19 previously, that the diesel cycle has a lower efficiency running on syngas than it does on biogas. Indeed, when we examine the heat output from the diesel engine, we find that the output from the gasification route is much higher than the biodigestion route.

However, not all this heat output from the engine is "free": both the biodigestion and gasification processes have various heating requirements. For biodigestion, this relates mainly to the maintenance of the biodigester at 37°C for optimal biological activity, and the penalty is rather small: 0.3 kW in the heat output. On the other hand, for the case of gasification, the gasifier needs a hefty amount of heat intake to run itself, in particular, because we chose to run the gasifier at a lower-than-usual air/fuel equivalence ratio. In addition, for the gasification process, because of the requirement that the feedstock into the gasifier must be reasonably dry (less than 15% moisture content), it will also take considerable amount of energy in the dryer to reduce the moisture content from the original 50% to 15%. In some studies, this energy is avoided by laying out the biomass out in the open to dry, using the low-quality heat from the air and sun. However, this process takes many days, and in an urban Lagos setting, is simply not feasible given the constrained land area. When summed up, this heating requirement for drying and running the gasification process turns out to be quite large: about 8.4 kW for our base case. This means that there is less net usable heat output from the gasification process as compared to the biodigestion process for our base case, at a given moisture content of 50%. We will discuss in greater depth about the dependency of the overall energy balance, in particular for the gasification process, on the moisture content later, but at this point, we conclude that for the typical municipal waste characteristics, biodigestion seems the more viable route from the energy conversion perspective.

Therefore, we can define and assign some system efficiencies to both processes by dividing the available power output by the initial fuel energy content: for gasification, at the given moisture content and feedstock conditions, this efficiency is about 12% for biodigestion, and 11% for gasification. Under different conditions, we expect these efficiencies to change, and the section immediately below will discuss some effects such as the initial feedstock variability, as well as the initial feedstock moisture content.

8.1 System Error Analysis

Earlier, we assessed the impact of variations in the characteristics of the input biomass feedstock (mainly in terms of the ultimate and structural analyses) on the fuel production, because, as explained previously, municipal waste is a highly heterogeneous mix of different biomass types that can change from day to day and season to season. The question we ask here is: given our inability to better characterize the waste composition in Lagos, what effect does this possible error has on the overall system performance? In this section, we analyze the case for both gasification and biodigestion.

8.1.1 Gasification Feedstock Sensitivity

As noted previously, the ultimate and structural analyses have a significant impact on the composition of the devolatilized gas, but this effect is quickly erased in the combustion zone, creating only a minor error (less than 2%). The more significant error actually comes from the differing gas/char yield for different types of biomass. There are two causes fro this variable gas/char yield in the different types of biomass: (a) different types of biomass have different structural components (lignin, hemicellulose, and cellulose), which decompose differently under pyrolyiss, and (b) different types of biomass have different amounts of inert ash, which serves to reduce the overall gas/char yield when such ash is included. The Cantera simulation results above suggest that at the typical range of pyrolysis gas yield

is around 0.6 to 0.8 initially, though of course, the composition of char also has an influence on how much syngas (of which variety) is produced.

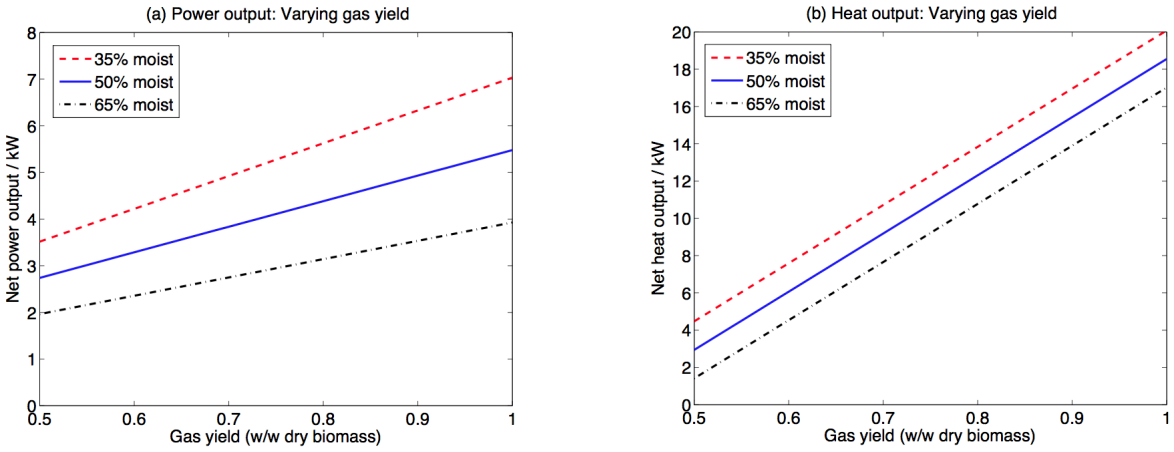

Figure 21: Sensitivity of the gasification system performance based on the initial feedstock conditions, which affect the fuel yield (a) The power output from gasification as a function of the gas yield. (b) The heat output from gasification as a function of the gas yield. The plots are done for different initial feedstock moisture contents of 35% (red), 50% (blue), and 65% (black).

Fig. 21(a) illustrates the effect of this uncertainty range on the net power output from the gasification system. It makes sense to observe that as the gas yield increases, the available power output also increases, because in our system, only gas, and not char, can contribute to useful work in the engine. Fig. 21(b) shows the effect of this uncertainty range on the net usable heat output from the gasification system. There is in reality a trade-off here: the higher the gas yield, the lower the heat contribution from the char. However, as the heat contribution from the char is already quite small in the base case (about 2.8 kW out of the total 19.6 kW of heat before the diesel engine), we surmise that the increasing heat contribution from the engine exhaust of burning syngas will be the more important factor. This is indeed true as Fig. 21(b) shows an increasing trend.

In all the figures above, we also plot the system performance based on three different initial moisture levels for the biomass feedstock. We will discuss this effect in a later section.

8.1.2 Biodigestion Feedstock Sensitivity

In this section, we perform some sensitivity analyses based on potential errors in the input feedstock for biodigestion. We first evaluate the impact of different types of feedstock on the fuel characteristics, which can then impact the power/heat output from the system.

With regard to biodigestion, there are two key uncertainties in the fuel production: (a) the fraction of methane in the biogas stream, and (b) the total biogas yield per unit mass of input feedstock. As explained in the process modeling results section before, both quantities may be affected by the characteristics of the input feedstock. Because municipal waste is mixed waste, it becomes very difficult to predict *a priori* the waste composition from the different biomass types. Therefore, it is important for us to analyze how this uncertainty affects the overall system performance, and evaluate whether or not such fluctuation in the power/heat output is acceptable for NovaGen.

As can be seen in Fig. 22(a), the net power output increases as the mole fraction of CH_4 increases, which is expected as the given volume of the gas contains increasing energy. While not shown in the plots, the diesel engine efficiency also increases from 25.4% to 26.2% over the parametric range. This corresponds, on the P-V diagram, to increasing temperatures T_2, T_3, and T_4 by about 10, 40, and 30 Kelvins respectively. Likewise, Fig. 22(b) illustrates that the net heat output also increases. While

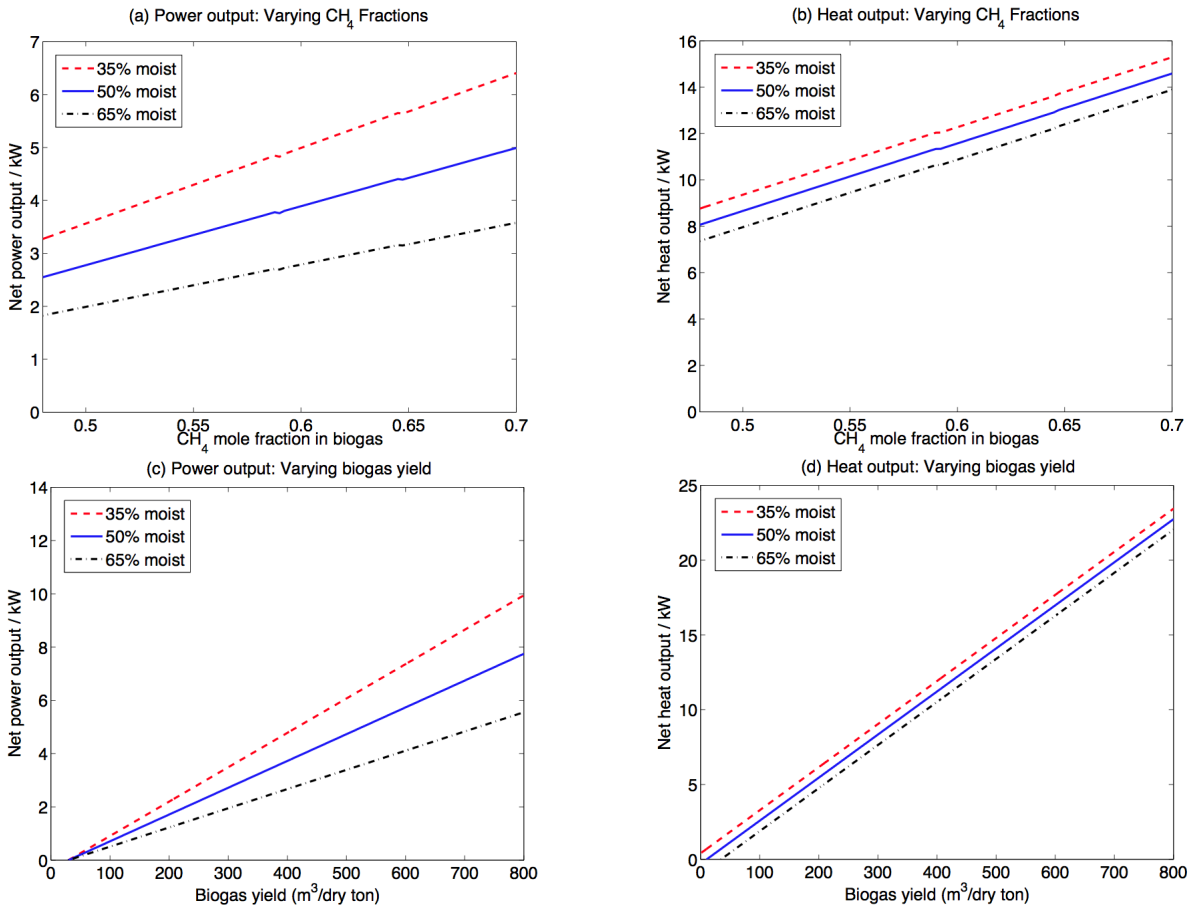

Figure 22: Sensitivity of the biodigestion system performance based on the initial feedstock conditions, which affect the fuel yield and/or composition. (a) The power output from biodigestion as a function of the CH_4 mole fraction of biogas. (b) The heat output from biodigestion as a function of the CH_4 mole fraction of biogas. (c) The power output from biodigestion as a function of the total biogas yield per dry unit mass of input feedstock. (d) The heat output from biodigestion as a function of the total biogas yield per dry unit mass of input feedstock. The plots are done for different initial feedstock moisture contents of 35% (red), 50% (blue), and 65% (black).

this figure plots the trends at three different moisture contents, we will discuss the influence of the initial feedstock moisture content later.

The other factor that varies as a function of feedstock characteristics is the overall biogas yield, measured in cubic meters per ton of dry biomass. As explained before, digested waste such as cow dung typically will have a low biogas yield, while high-fat and high-sugar wastes tend to have a higher biogas yield. Depending on the composition of the municipal waste, differing yields can be obtained.

Fig. 22(c) examines the dependency of the power output from the system on this factor, by varying the biogas yield from near zero to 800 m^3/dry ton of initial biomass. It should be noted that there is a minimally viable gas yield value at 30^3/dry ton, below which the system will be unable to produce net positive work. 22(d) shows the same for the available heat output from the system, and we see that the heat output is much more sensitive to the changes in biogas yield compared to the power output.

8.2 Effect of Moisture Content

While for the base case, we used a value of 50% (wet basis) moisture content for the incoming municipal waste from Lagos, we recognize that this value can vary greatly, dependent upon the waste composition, neighborhood, weather, and season. To understand the impact of this variable on the overall system performance, in Figures 21 and 22 previously, we also plotted the anticipated system performance based on two other moisture values for the initial biomass: 35% and 65% (again wet basis), assuming a constant incoming mass flow rate (i.e. gasifier/biodigester feeding rate). We can see that for both gasification and biodigestion, the net power available is affected significantly by this varying moisture content: a higher moisture content leads to a lower value for the net power available. This is expected for several reasons. Firstly, per unit of mass flow of incoming municipal waste, there is now less organic waste that actually contributes to the fuel conversion process, which affects how much fuel goes into the diesel engine. Secondly, in processes that require water removal (for example, biodigestion), the higher moisture content means a larger separation cost. It is noted that the presence of larger moisture content will also affect the amount of steam available inside the gasifier, which will also affect the reactions dictating the formation of H_2 and CO. Typically, we expect the formation rate to increase as a function of increasing steam concentration inside the reduction zone, with a greater preference for H_2. However, as the plot shows, this positive effect is overpowered by the two previous negative effects.

In contrast, the right panels of Figures 21 and 22 show trends of a somewhat different characteristic. Notably, in contrast to the power output, the slopes of the available heat output do not seem to depend on the moisture content. This can be understood by noting that for gasification, the higher the initial moisture content, the more drying is required to bring the biomass down to acceptable moisture contents to feed into the gasifier. The removal of an additional 15% moisture corresponds to an offset of about 1.53 kW in the heat requirement. For biodigestion, while the moisture level does impact the available heat output, we see that this effect is much smaller. This makes sense, as biodigestion does not require the moisture to be heated and removed from the biomass completely, but rather, that the whole biomass/water mixture be brought from ambient temperature to 37°C where the biodigestino takes place.

If it is true, as discussed above, that the initial moisture within the biomass levies such a big energy penalty on the gasification process, then we expect that if we reduce the moisture content, gasification will become increasingly attractive in comparison with biodigestion, until a point where it becomes energetically superior. By performing sensitivity analysis on the system, we found out that this point is around 15% moisture content, which, incidentally, is also the upper maximum intake moisture content designed for various types of gasification units. This is interesting, as it tells that most gasifiers seem already designed with this energetic constraint in mind. While this moisture content is readily achievable with post-harvest typical agricultural waste—which are plenty in rural Nigeria—in practice it is difficult to achieve with solely municipal waste, which typically has a much higher moisture content unless household-based segregation based on moisture level were to take place. While it is possible to reduce the heating requirement in the gasification pathway by letting the biomass dry using lower-quality heat, such as the sun or the ambient air, this strategy requires a very large land area and may be weather-dependent. In an urban setting such as Lagos, its feasibility is also questionable.

9 Conclusion and Discussions

9.1 Summary

In this study, we undertook an assessment of biodigestion and gasification of municipal solid waste in the context of an upscale apartment complex in Lagos. To do this, we created models for both pro-

cesses. We first elucidated the underlying kinetics and molecular balance that govern fuel production, and evaluated how variations in the input biomass may impact this result. We then integrated these insights into a macroscopic systems-level model of both processes in order to account for the overall energy balance and efficiency. Here are some key insights from our study:

1. Both producer gas and biogas production is variously sensitive to the input feedstock characteristics, in particular, the ultimate analysis and structural data. For gasification, this affects the overall gas yield without significantly changing the gas composition. For biodigestion, the different types of feedstock will alter the methane fraction as well as the overall biogas yield; however, the sensitivity is comparatively low in this case.

2. There are two modes of running the diesel engine: pre-mixing the fuel and air before compression, or injecting the fuel after compression. Having evaluated both cases, we concluded that the first mode yields superior efficiency. For producer gas, the engine efficiency is around 23 %, while for biogas, 26%.

3. The pretreatment and post-treatment processes in both gasification and biodigestion do not impose a significant energy penalty on the system performance (less than 5%). This may be due to our idealized model, which we will discuss in the subsequent section.

4. The first-law efficiency for the full system—defined as the fraction of work extracted to the overall calorific content of the incoming organic waste—is comparable for both conversion techniques at 11-12%. At this level, the power output is about 3.6-3.8 kW, which is sufficient for the average case of 3 kW for the households. However, it will not meet the upper bound of 8 kW of household electricity demand.

5. At the given waste moisture content and treatment conditions, there is more available exhaust heat for biodigestion which, while not of primary importance to NovaGen, can nonetheless be utilized in other ways by the households, such as heating shower water.

6. Both processes show significant sensitivity to the initial feedstock moisture content. A lower moisture content generally leads to higher energy yields, especially for the case of gasification. In fact, gasification will be energetically comparable to biodigestion at an initial feedstock moisture content of about 15 %, unless alternative drying strategies using lower quality heat (such as the sun) are employed.

7. Because municipal waste is highly mixed, we expect daily or seasonal fluctuations to have a significant impact on the system-level energy performance. This fluctuation should not be overlooked and NovaGen should seek to characterize it as accurately as possible.

Overall, should NovaGen proceed with either waste conversion techniques? As concluded above, if NovaGen is only interested in the power output, then both gasification and biodigestion may be feasible at a power output of 3 kW. If NovaGen seeks to satisfy the upper estimate of 8 kW for the community, then additional energy sources—such as additional food waste, diesel, or solar sources—should be sought. From the point of view of overall energy balance including the possible utility of waste heat from the diesel cycle, we recommend biodigestion.

From the analysis above, we arrive at the following figures:

Table 10: Results summary

Scenario	Business as usual	Biodigestion	Gasification
1st law efficiency	20%	12%	11%
Food waste used	0%	100%	100%
Diesel use avoided (l/year)	0	5548	5256
Fuel cost savings (USD)	0	5216.4	5506.3

The savings above reflect only fuel cost savings. In reality, a lifecycle analysis should consider other savings such as landfill tipping cost, and the transportation of the diesel and waste.

We do not have the exact figures for the capital cost of either hardware. However, if we use the baseline approximation for gasification which is USD 1/W, given our community capacity, we expect such a unit to cost about USD 8000, excluding peripheral facilities such as dryers, scrubbers, etc. This would imply a return on investment of approximate 2-3 years.

9.2 Assumptions and Limitations

Throughout the modeling process, we made various simplifications in both the biodigestion and gasification processes. In this section, we enumerate these assumptions which are bases for future work.

Gasification

1. The gas / char yield is evaluated using a single-particle model. This is a highly simplified kinetic model since, in reality, the interaction between the particles themselves is likely to be significant for a packed bed.

2. As mentioned before, ensuring good heat exchange between the exhaust and the gasifier may not be practically feasible. Therefore, for this system, the equivalence ratio should be much higher which will consequently increase the Nitrogen mole fraction in the producer gas. This could present potential problems for ignition and NOx control in the IC engine and may, therefore, have to be separated out. This separation will result in an efficiency penalty.

3. It is assumed that the char concentration in the reduction zone is *sufficiently high* so that the heterogeneous chemical reactions are not controlled by the char concentration in the bed. This simplification may not hold true for higher equivalence ratios (more char gets burnt).

4. The current analysis has not assumed any post-treatment to the gas. While the menace of emissions and their control has been somewhat described in Section (4.1.1), incorporating separation units will result in further efficiency penalty.

5. Due to limited scope of this study, we prescribed a temperature profile inside the gasification reactor based on typical experimental data, instead of building a full-fledged downdraft reactor model and letting the energy balance dictate the temperature profile.

6. The system-level analysis did not account for the fate of ash, which is expected to accumulate and may need transportation to be removed from the site.

Biodigestion

1. We did not use a kinetics or steady-state modeling approach for biodigestion, and assume a well-define efficiency for a global reaction. In further studies, a more detailed implementation for the biodigestion process—such as the ADM1 model—is warranted in order to better assess the reactor behavior under different feedstock and temperature conditions.

2. We did not account for the water cycle. In a typical biodigestion process, a large amount of water is added to the input feedstock to form a slurry-like consistency before being fed into the biodigester. In our modeling, we did not account for this water as it has minimal impact on the overall system energy balance. However, in more realistic models, we will need to account for various steps such as water pumping, water extraction from the wet digestate, and so forth.

3. We did not account for additional work required to keep the biodigester well-mixed, for example, the constant stirring that is found in various installations.

4. We did not trace the fate of the solid digestate in the biodigestion process. In many biodigestion plants, this digestate is used for fertilizer on site or in nearby farms. In others, it is discarded. However, in either case, there is typically an energy requirement related to the transport of this substance, which we did not explicitly include in the model.

Finally, there are some simplifications which are common for both conversion strategies:

1. We did not account for any heat losses in the different processes in both biodigestion and gasification. In reality, these heat losses may add up to significant penalties in the system-level energy balance.

2. Typically, a 10% diesel is necessary in order to operate the diesel engine with biogas or producer gas. However, for the interest of system energy balance, we only accounted for biogas and producer gas in the flowsheet, and ignored the diesel from the system.

References

[1] Rudolf Braun. Anaerobic digestion: a multi-faceted process for energy, environmental management and rural development. *Improvement of Crop Plants for Industrial End Uses*, (335-416), 2007.

[2] Mustafa Balat. Production of bioethanol from lignocellulosic materials via the biochemical pathway: a review. *Energy Conversion and Management*, 52(2):858–875, 2011.

[3] Anaerobic digestion of municipal solid waste: A modern waste disposal option on the verge of breakthrough. *Biomass and Bioenergy*, 9(1-5):365–376, 1995.

[4] Carlo N. Hamelinck, Geertje van Hooijdonk, and Andre PC Faaij. Ethanol from lignocellulosic biomass: techno-economic performance in short-, middle- and long-term. *Biomass and Bioenergy*, 28(4):384–410, 2005.

[5] UN FAO. Global food losses and food waste. Technical report, 2011.

[6] Ityona Amber, Daniel M. Kulla, and Nicholas Gukop. Municipal waste in nigeria generation, characteristics and energy potential of solid. *ASIAN JOURNAL OF ENGINEERING, SCIENCES AND TECHNOLOGY*, 2012.

[7] Peter McKendry. Energy production from biomass (part 2): conversion technologies. *Bioresource Technology*, 83(1):47 – 54, 2002. Reviews Issue.

[8] A.A. Khan, W. de Jong, P.J. Jansens, and H. Spliethoff. Biomass combustion in fluidized bed boilers: Potential problems and remedies. *Fuel Processing Technology*, 90(1):21 – 50, 2009.

[9] Ayhan Demirbas. Potential applications of renewable energy sources, biomass combustion problems in boiler power systems and combustion related environmental issues. *Progress in Energy and Combustion Science*, 31(2):171 – 192, 2005.

[10] Thomas Nussbaumer. Combustion and co-combustion of biomass: Fundamentals, technologies, and primary measures for emission reduction. *Energy & Fuels*, 17(6):1510–1521, 2003.

[11] Bernd R.T Simoneit. Biomass burning a review of organic tracers for smoke from incomplete combustion. *Applied Geochemistry*, 17(3):129 – 162, 2002.

[12] L.S. Johansson, C. Tullin, B. Leckner, and P. Sjvall. Particle emissions from biomass combustion in small combustors. *Biomass and Bioenergy*, 25(4):435 – 446, 2003.

[13] R. Saidur, E.A. Abdelaziz, A. Demirbas, M.S. Hossain, and S. Mekhilef. A review on biomass as a fuel for boilers. *Renewable and Sustainable Energy Reviews*, 15(5):2262 – 2289, 2011.

[14] Thomas R. Miles, Thomas R. Miles Jr, Larry L. Baxter, Richard W. Bryers, Bryan M. Jenkins, and Laurance L. Oden. Boiler deposits from firing biomass fuels. *Biomass and Bioenergy*, 10(23):125 – 138, 1996. Strategic Benefits of Biomass and Wasteful fuels.

[15] Ajay Kumar, David D. Jones, and Milford A. Hanna. Thermochemical biomass gasification: A review of the current status of the technology. *Energies*, 2(3):556–581, 2009.

[16] Mustafa Balat, Mehmet Balat, Elif Kirtay, and Havva Balat. Main routes for the thermoconversion of biomass into fuels and chemicals. part 1: Pyrolysis systems. *Energy Conversion and Management*, 50(12):3147 – 3157, 2009.

[17] E. Bocci, M. Sisinni, M. Moneti, L. Vecchione, A. Di Carlo, and M. Villarini. State of art of small scale biomass gasification power systems: A review of the different typologies. *Energy Procedia*, 45(0):247 – 256, 2014. {ATI} 2013 - 68th Conference of the Italian Thermal Machines Engineering Association.

[18] Peter McKendry. Energy production from biomass (part 3): gasification technologies. *Bioresource Technology*, 83(1):55 – 63, 2002. Reviews Issue.

[19] Ian Narvaez, Alberto Orio, Maria P. Aznar, and Jose Corella. Biomass gasification with air in an atmospheric bubbling fluidized bed. effect of six operational variables on the quality of the produced raw gas. *Industrial & Engineering Chemistry Research*, 35(7):2110–2120, 1996.

[20] P. Ollero, A. Serrera, R. Arjona, and S. Alcantarilla. The {CO2} gasification kinetics of olive residue. *Biomass and Bioenergy*, 24(2):151 – 161, 2003.

[21] S. Rapagna, N. Jand, A. Kiennemann, and P.U. Foscolo. Steam-gasification of biomass in a fluidised-bed of olivine particles. *Biomass and Bioenergy*, 19(3):187 – 197, 2000.

[22] Lijun Wang, Curtis L. Weller, David D. Jones, and Milford A. Hanna. Contemporary issues in thermal gasification of biomass and its application to electricity and fuel production. *Biomass and Bioenergy*, 32(7):573 – 581, 2008.

[23] C. Lucas, D. Szewczyk, W. Blasiak, and S. Mochida. High-temperature air and steam gasification of densified biofuels. *Biomass and Bioenergy*, 27(6):563 – 575, 2004. Pellets 2002. The first world conference on pellets.

[24] Emanuele Graciosa Pereira, Jadir Nogueira da Silva, Jofran L. de Oliveira, and Cssio S. Machado. Sustainable energy: A review of gasification technologies. *Renewable and Sustainable Energy Reviews*, 16(7):4753 – 4762, 2012.

[25] Lopamudra Devi, Krzysztof J Ptasinski, and Frans J.J.G Janssen. A review of the primary measures for tar elimination in biomass gasification processes. *Biomass and Bioenergy*, 24(2):125 – 140, 2003.

[26] Carin Myren, Christina Hrnell, Emilia Bjrnbom, and Krister Sjstrm. Catalytic tar decomposition of biomass pyrolysis gas with a combination of dolomite and silica. *Biomass and Bioenergy*, 23(3):217 – 227, 2002.

[27] Douglas C. Elliott, L. John Sealock, and Eddie G. Baker. Chemical processing in high-pressure aqueous environments. 2. development of catalysts for gasification. *Industrial & Engineering Chemistry Research*, 32(8):1542–1548, 1993.

[28] Mohammad Asadullah, Shin ichi Ito, Kimio Kunimori, Muneyoshi Yamada, and Keiichi Tomishige. Biomass gasification to hydrogen and syngas at low temperature: Novel catalytic system using fluidized-bed reactor. *Journal of Catalysis*, 208(2):255 – 259, 2002.

[29] J.A. Ruiz, M.C. Jurez, M.P. Morales, P. Muoz, and M.A. Mendvil. Biomass gasification for electricity generation: Review of current technology barriers. *Renewable and Sustainable Energy Reviews*, 18(0):174 – 183, 2013.

[30] Yukihiko Matsumura, Tomoaki Minowa, Biljana Potic, Sascha R.A. Kersten, Wolter Prins, Willibrordus P.M. van Swaaij, Bert van de Beld, Douglas C. Elliott, Gary G. Neuenschwander, Andrea Kruse, and Michael Jerry Antal Jr. Biomass gasification in near- and super-critical water: Status and prospects. *Biomass and Bioenergy*, 29(4):269 – 292, 2005.

[31] Samsudin Anis and Z.A. Zainal. Tar reduction in biomass producer gas via mechanical, catalytic and thermal methods: A review. *Renewable and Sustainable Energy Reviews*, 15(5):2355 – 2377, 2011.

[32] S. Dasappa N. H. Ravindranath, H. I. Somashekar and C. N. Jayasheela Reddy. Sustainable biomass power for rural india: Case study of biomass gasifier for village electrification. *Current Science*, 87, 2004.

[33] Buljit Buragohain, Pinakeswar Mahanta, and Vijayanand S. Moholkar. Biomass gasification for decentralized power generation: The indian perspective. *Renewable and Sustainable Energy Reviews*, 14(1):73 – 92, 2010.

[34] Z.A Zainal, Ali Rifau, G.A Quadir, and K.N Seetharamu. Experimental investigation of a downdraft biomass gasifier. *Biomass and Bioenergy*, 23(4):283 – 289, 2002.

[35] V. Belgiorno, G. De Feo, C. Della Rocca, and R.M.A. Napoli. Energy from gasification of solid wastes. *Waste Management*, 23(1):1 – 15, 2003.

[36] Avdhesh Kr. Sharma. Experimental study on 75kwth downdraft (biomass) gasifier system. *Renewable Energy*, 34(7):1726 – 1733, 2009.

[37] Avdhesh Kr. Sharma. Experimental investigations on a 20 kwe, solid biomass gasification system. *Biomass and Bioenergy*, 35(1):421 – 428, 2011.

[38] Pratik N. Sheth and B.V. Babu. Experimental studies on producer gas generation from wood waste in a downdraft biomass gasifier. *Bioresource Technology*, 100(12):3127 – 3133, 2009.

[39] Francisco V. Tinaut, Andrs Melgar, Juan F. Prez, and Alfonso Horrillo. Effect of biomass particle size and air superficial velocity on the gasification process in a downdraft fixed bed gasifier. an experimental and modelling study. *Fuel Processing Technology*, 89(11):1076 – 1089, 2008.

[40] Rajeev M. Jorapur and Anil K. Rajvanshi. Development of a sugarcane leaf gasifier for electricity generation. *Biomass and Bioenergy*, 8(2):91 – 98, 1995.

[41] Murat Dogru, Adnan Midilli, and Colin R Howarth. Gasification of sewage sludge using a throated downdraft gasifier and uncertainty analysis. *Fuel Processing Technology*, 75(1):55 – 82, 2002.

[42] Maria Puig-Arnavat, Joan Carles Bruno, and Alberto Coronas. Review and analysis of biomass gasification models. *Renewable and Sustainable Energy Reviews*, 14(9):2841 – 2851, 2010.

[43] S. Jarungthammachote and A. Dutta. Thermodynamic equilibrium model and second law analysis of a downdraft waste gasifier. *Energy*, 32(9):1660 – 1669, 2007.

[44] Niladri Sekhar Barman, Sudip Ghosh, and Sudipta De. Gasification of biomass in a fixed bed downdraft gasifier a realistic model including tar. *Bioresource Technology*, 107(0):505 – 511, 2012.

[45] D.L. Giltrap, R. McKibbin, and G.R.G. Barnes. A steady state model of gas-char reactions in a downdraft biomass gasifier. *Solar Energy*, 74(1):85 – 91, 2003.

[46] B.V. Babu and Pratik N. Sheth. Modeling and simulation of reduction zone of downdraft biomass gasifier: Effect of char reactivity factor. *Energy Conversion and Management*, 47(1516):2602 – 2611, 2006.

[47] T.H. Jayah, Lu Aye, R.J. Fuller, and D.F. Stewart. Computer simulation of a downdraft wood gasifier for tea drying. *Biomass and Bioenergy*, 25(4):459 – 469, 2003.

[48] Eliseo Ranzi, Michele Corbetta, Flavio Manenti, and Sauro Pierucci. Kinetic modeling of the thermal degradation and combustion of biomass. *Chemical Engineering Science*, 110:2 – 12, 2014.

[49] Carlos R. Altafini, Paulo R. Wander, and Ronaldo M. Barreto. Prediction of the working parameters of a wood waste gasifier through an equilibrium model. *Energy Conversion and Management*, 44(17):2763 – 2777, 2003.

[50] Avdhesh Kr. Sharma. Modeling fluid and heat transport in the reactive, porous bed of downdraft (biomass) gasifier. *International Journal of Heat and Fluid Flow*, 28(6):1518 – 1530, 2007. Revised and extended papers from the 5th conference in Turbulence, Heat and Mass Transfer The 5th conference in Turbulence, Heat and Mass Transfer.

[51] Maria Puig Arnavat. *Performance modelling and validation of biomass gasifiers for trigeneration plants*. PhD thesis, Universitat Rovira i Virgili, 2011.

[52] W. Boie. Fuel technology calculations. *Energietechnik*, 3:309–16, 1953.

[53] Richard B. Bates and Ahmed F. Ghoniem. Biomass torrefaction: modeling of reaction thermochemistry. *Bioresource Technology*, 134:331–340, 2013.

[54] A.C. Kent, H.N. Rosen, and B.M. Hari. Determination of equilibrium moisture content of yellow-poplar sapwood above 100c with the aid of an experimental psychrometer. *Wood Science and Technology*, 15(93), 1981.

[55] S.S. Alves and J.F. Figueiredo. A model for pyrolysis of wet wood. *Chemical Engineering Science*, 12:2861–2869, 1989.

[56] Marcelis Jacob Cornelis van der Stelt. *Chemistry and Reaction Kinetics of Biowaste Torrefaction*. PhD thesis, Technical University of Eindhoven, 2010.

[57] Mohammad J Taherzadeh and Keikhosro Karimi. Pretreatment of lignocellulosic wastes to improve ethanol and biogas production: a review. *International Journal of Molecular Sciences*, 9(9):1621–1651, 2008.

[58] Heidi Berg. Comparison of conversion pathways for lignocellulosic biomass to biofuel in mid-norway. *Thesis - Master of Energy and Environmental Engineering*, 2013.

[59] Z. Miao et al. Energy requirement for comminution of biomass in relation to particle physical properties. *Industrial Crops and Products*, 33(2):504–513, 2011.

[60] Nathan Curry and Pragasen Pillay. Biogas prediction and design of a food waste to energy system for the urban environment. *Renewable Energy*, 41(0):200 – 209, 2012.

[61] Effect of engine parameters and type of gaseous fuel on the performance of dual fuel gas diesel engines - a critical review. *Renewable and Sustainable Energy Reviews*, 13(6-7):1151–1184, 2009.

[62] O Badr, G.A Karim, and B Liu. An examination of the flame spread limits in a dual fuel engine. *Applied Thermal Engineering*, 19(10):1071 – 1080, 1999.

[63] Ityona Amber, Daniel M. Kulla, and Nicholas Gukop. Municipal waste in nigeria: generation, characteristics, and energy potential of solid. *Asian Journal of Engineering, Sciences, and Technology*, 2(2), 2012.